(2)

GNUGNOL1

NUREG/CR-1138
PNL-3207
RE

Diffusion and Exhalation of Radon from Uranium Tailings

W. B. Silker
P. G. Heasler

Laura E. Santos, NRC Project Manager

October 1979

Prepared for
the U.S. Nuclear Regulatory Commission

Pacific Northwest Laboratory
Operated for the U.S. Department of Energy
by Battelle Memorial Institute

Battelle

PNL-3207

NUREG/CR-1138
PNL-3207
RE

DIFFUSION AND EXHALATION OF RADON FROM URANIUM TAILINGS

W. B. Silker
P. G. Heasler

Laura E. Santos, NRC Project Manager

October, 1979

Prepared for
the U. S. Nuclear Regulatory Commission
under a Related Services Agreement
with the U. S. Department of Energy
under Contract EY-76-C-06-1830
Fin. No. B-2269

Pacific Northwest Laboratory
Richland, Washington 99352

DOE- Richland, WA

TABLE OF CONTENTS

FIGURES

TABLES

DIFFUSION AND EXHALATION OF RADON FROM URANIUM TAILINGS

EXECUTIVE SUMMARY

The objectives of this program were to develop and apply an absolute method for determining radon emissions from uranium tailings. Briefly, ^{226}Ra and ^{222}Rn (^{214}Pb) concentration gradients as a function of depth were measured in situ by gamma-ray spectrometry, which was accomplished by lowering a calibrated intrinsic germanium detector to discrete levels within a sealed and cased test well hole and accumulating the gamma-ray spectrum with a multichannel analyzer. Differences between the vertical distributions of radium and radon were used to calculate a radon diffusion coefficient, the fraction of emanating radon and the flux of radon across the tailings-air interface. A diffusional model was developed that accounted for the non-uniform radium concentrations that occur with depth in tailings piles.

From extensive field measurements, conducted at tailings piles resulting from alkaline and acid leach processes, the following averaged radon emanation (α) and diffusion (D) coefficients were determined for areas of differing moisture content and composition.

	Alkaline Leach		Acid Leach	
	α	D cm^2/sec	α	D cm^2/sec
Wet beach	0.36	0.0010	0.20	0.0027
Dry beach	0.43	0.0040	0.19	0.0037
Berm	0.40	0.015	0.12	0.017

Higher rates of diffusion occurred at the berms, which are comprised of the coarsest tailings material and are the driest portions of the tailings piles. Diffusion rates successively decreased in dry and wet beach areas. Roughly 40% of the radon production in the more finely ground alkaline leach tailings was free to diffuse, compared to 20% in the acid leach material.

Rates of radon exhalation as determined by the developed diffusional model were verified by mass balance of the total radium and radon existing in the tailings column. Averaged radon fluxes of 80, 260, and 320 atoms/

$cm^2 \cdot sec$ were determined for wet beach, dry beach, and berm areas of the alkaline leach tailings, and 60, 190, and 180 atoms/$cm^2 \cdot sec$ for comparable areas of acid leach tailings. These fluxes result in a calculated areal emission rate for radon of about 7 Ci/day/km^2 for both of the acid and alkaline leach tailings piles employed in this study.

Radon fluxes determined concomitantly by charcoal canister adsorption averaged 30% higher than those determined by the diffusion model. Variations of a factor of two in the measured radon flux were observed for identically exposed canisters. Increasing exposure periods of a canister generally resulted in reduced estimates of the radon flux.

Changes of barometric pressure and periods of high local winds did not significantly alter the flux of radon across the tailings-air interface.

Measurements were conducted at vegetated and barren sites in close proximity on an abandoned tailings pile. Radon flux from the vegetated site was nearly double that found at the non-vegetated location.

INTRODUCTION

Uranium mill tailings present a source of concern due to the potential radiological exposure of local population resulting from the emanation of radon and the subsequent production of its radioactive daughters. Radon-222*, a daughter of ^{226}Ra**, is a member of the natural decay chain originating with ^{238}U, and as such, is present in near equilibrium concentrations in uranium ore. The milling process separates uranium from the other members of the decay chain, which are disposed with the spent feed material to a tailings pile. Radon can be produced in or diffuse into the interstitial pores of the tailings column and, being a noble gas, can then diffuse upward through the column and ultimately enter the atmosphere. An excellent review of literature describing radon migration and parameters influencing its diffusion is given by Tanner[1,2] and will not be detailed in this report.

Any assessment of the radiological impact of radon exhaled from a uranium mill tailings pile requires knowledge of its rate of release and the influence of various physical and meteorological parameters on this rate. A variety of approaches have been used to evaluate the quantities of radon released to the atmosphere, both from specific sites and from general soil areas, most of which involve collection and subsequent analysis of radon or radon daughters at or above the soil surface. A common method involves accumulation of exhaled radon in a container sealed to the soil surface followed by removal of an aliquot for radon analysis.[3,4] Countess[5] and Megumi and Mamuru[6] describe methods by which exhaled radon is accumulated directly by adsorption onto activated charcoal and quantified by gamma-ray spectrometric analyses of radon daughters. Other investigators, e.g.,[7,8], have determined the radon or radon daughter inventories in the air column and have used these data to estimate the regional flux of radon across the soil-air interface.

While these techniques afford useful data regarding instantaneous exhalation of radon, they provide little or no information on temporal variations of radon exhalation or diffusional characteristics of radon within

*Hereinafter called "radon"
**Hereinafter called "radium"

the soil column. Kraner, et al[3] determined the radon concentration in soil gas sampled from various depths within the soil column and were thus able to calculate a radon diffusion coefficient and the rate of exhalation of radon from the soil surface. We took a more mechanistic approach, basically measuring the changes of concentration of radium and radon, as its ^{214}Pb daughter, as a function of depth in the soil column by in-situ gamma-ray spectrometry. From the rate of change of parent-daughter concentrations with depth, the rates of radon diffusion and exhalation were calculable.[13]

FIELD SITES

Tailings piles at two uranium mills in the Grants, New Mexico area were selected for this study as representative of acid and carbonate leach processes employed by the U. S. uranium milling industry. The United Nuclear-Homestake Partners (UN-HP) mill employs a carbonate leach process to extract uranium from about 3500 tonnes per day of ore that has been crushed and milled so that 5% is +48 mesh and 38% is -200 mesh. The residual from the leach process, comprising the total bulk of ore and essentially all of the radium originally present, is transported as a slurry to the tailings pile. Coarse particulates are removed by a cyclone separator and used to continually elevate the berm containing the pile; the remaining fines and aqueous waste are disposed to the center of the tailings pile.

This tailings pile is situated above grade and after about twenty years of operation is now approximately 600 m wide, 1400 m long, and 25 m high (Fig. 1). It is divided roughly into two halves, each of which alternately receives tailings material from the mill. Measurements for this study were conducted in the standby side of the tailings pile which, including the sides, presented a surface area of 0.46 km^2 to the atmosphere. At the time of measurements, residual water covered an area of about 0.01 km^2 at the center of the standby side, and soil moisture content decreased with distance to the sides of the pile. The areas of wet beach, dry beach, and berm covered surfaces of 0.05, 0.34, and 0.6 km , respectively. There is also an unused tailings pile on this property that resulted from an old alkaline leach process mill that was operated in the 1950's prior to start-up of the current mill. These tailings, representing the pentagonal area in Fig. 1, are also deposited above grade to a depth of about 3 m and cover an area of about 0.3 km^2.

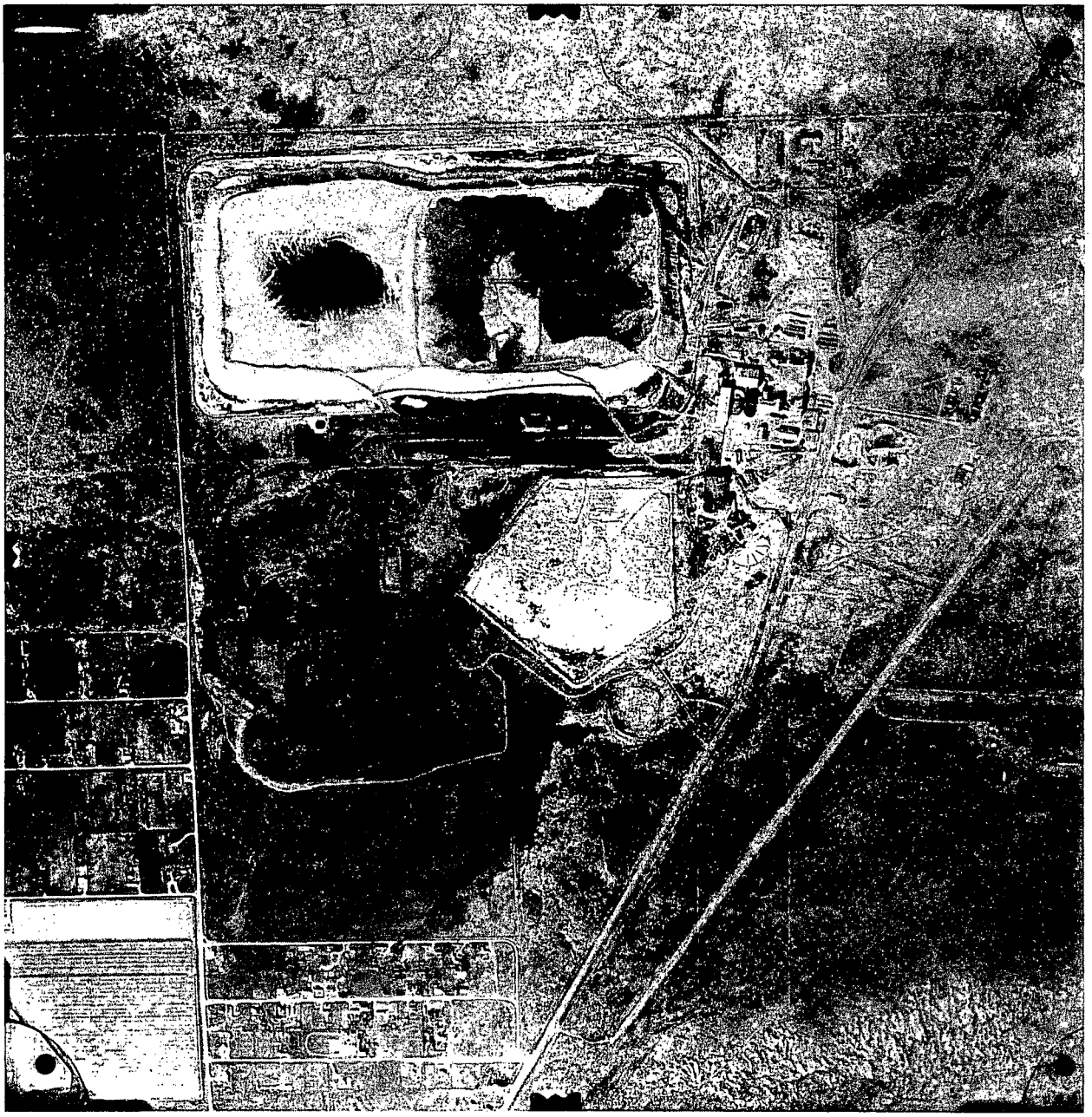

FIGURE 1. United Nuclear-Homestake Partners Mill, Grants, New Mexico

The Kerr-McGee Nuclear Corp. mill at Ambrosia Lake, New Mexico, uses a sulfuric acid leach to extract uranium from about 7000 tonnes per day of uranium ore. Ore for the acid leach mill is ground so that ∿30% is +48 mesh and 16% is -200 mesh, thus providing a coarser feed than that required for a carbonate leach process. Mill tailings are slurried to a tailings disposal pond (Fig. 2) and are discharged to the outer edge of the disposal area. Gravity settling results in deposition of larger particulates nearer the periphery of the tailings pile with transport of fines toward the center. The containment berm of this tailings pile is maintained by bulldozing material from inside the pile to elevate the dike. Solution covered about 0.29 km^2 of the 1.1 km^2 area of this tailings pile and the areal extents of wet beach, dry beach, and berm were roughly 0.11, 0.46, and 0.25 km^2, respectively.

LOCATION AND IMPLANTATION OF TEST HOLES

Test holes were implanted at locations on the tailings piles that were originally selected as representative of the existing soil and moisture conditions. When the tailings conditions permitted, a 15.2 cm diameter Schedule 40 PVC pipe, with a well point sealed on one end, was forced by impaction to the desired sampling depth, usually between 1.5 and 3.0 m below the tailings surface. Under other conditions, an undersized hole was predrilled into the tailings with a post hole auger and the PVC pipe was forced to the bottom of the hole. In all cases, the PVC pipe was sealed to prevent intrusion of either water or soil gas. It was imperative to eliminate any air voids between the outside of the pipe and the soil to prevent flow channeling of soil gases that would perturb normal radon transport. Intimate contact of tailings and the casing was assured at those locations where the test holes were impacted directly into the tailings. At locations where predrilled holes were employed, water was directed down the outside of the pipe to collapse tailings material into any air voids that may have existed between the pipe and the tailings. No evidence of air voids was detected experimentally in any of the subsequent measurements made to determine radionuclide concentration profiles.

Test holes were implanted in the standby side of the UN-HP tailings pile at locations shown in Fig. 3, which were selected to characterize

FIGURE 2. Kerr-McGee, Ambrosia Lake, New Mexico

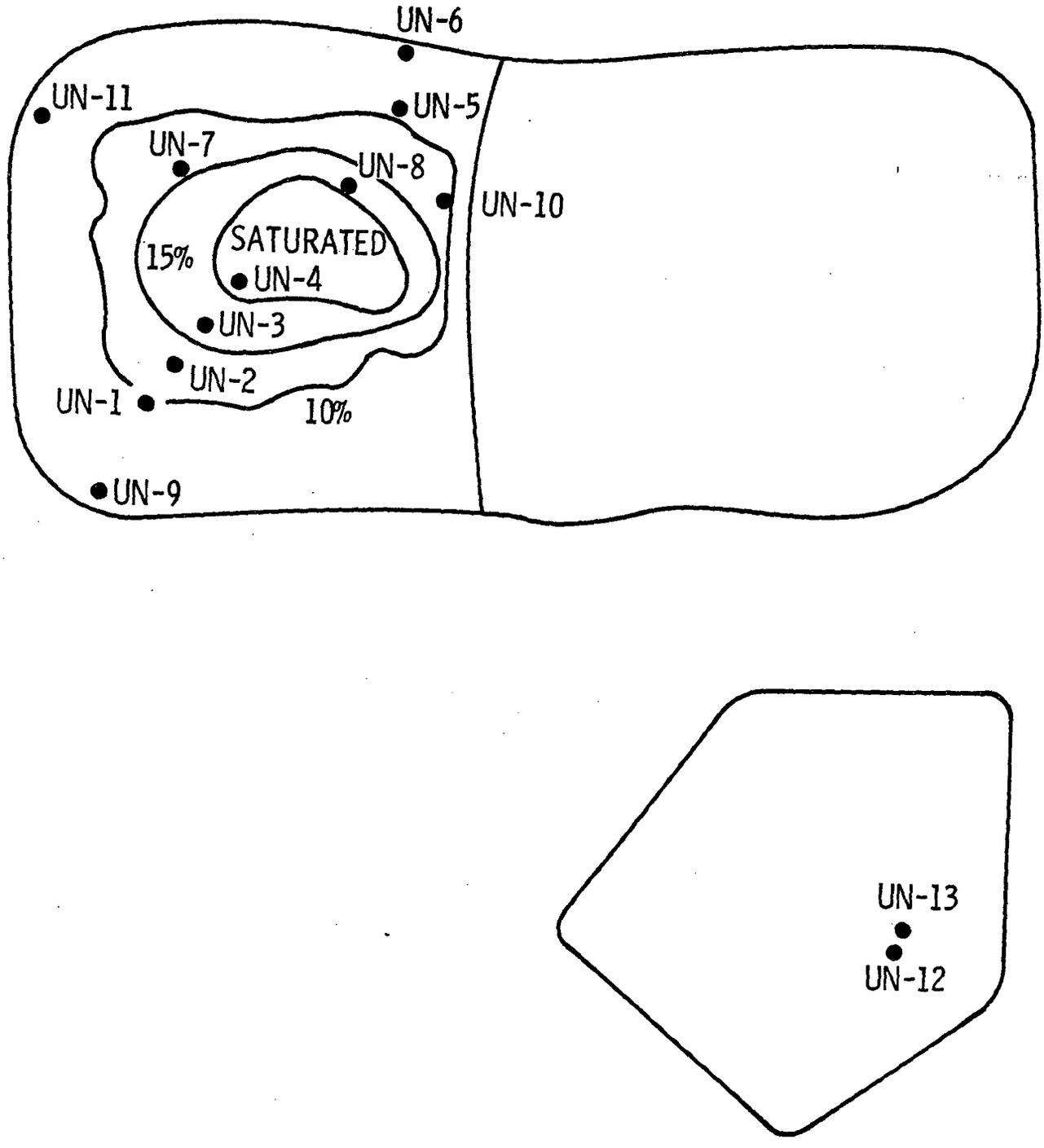

FIGURE 3. Test Locations at the UN-HP Tailings Pile

radon diffusion parameters within the approximate surface soil moisture isopleths depicted. Three test holes, UN-6, -9, and -11, were located on the outside slope of the berm; UN-1, -2, -5, and -10 at locations designated as dry beach; UN-3, -7, and -8 within the wet beach area; and UN-4 in the saturated area covered with standing water. In the course of normal operation, tailings from the mill were directed to the side of the tailings pile in which our test holes were located. The casings were extended on several of the test holes to prevent their burial and preserve the facilities for future measurements. Those locations where measurements were conducted after deposition of approximately two additional meters of tailings are subsequently designated with a "B" following the hole identification. Two test holes were implanted in the abandoned tailings pile on the UN-HP property (Fig. 3) within 40 m of each other, and presumably in tailings of comparable composition. The hole at UN-13 was in an area that had been sparsely revegetated with Four-wing Saltbush (*Atriplex canescens*), while UN-12 was located in an area devoid of vegetation.

Test holes at the Kerr-McGee tailings pile were all implanted into predrilled holes because the coarser tailings material would not yield to impaction methods. The test locations shown in Fig. 4 again were selected to accomodate differences in the soil types and moisture regimes present. Locations KM-1 and KM-5 were originally implanted adjacent to standing water on stabilized tailings that formed a solid sand beach. The distribution of water at the Kerr-McGee tailings pile was found to have been significantly altered when we returned in May, 1979. At this time, standing water had receded sufficiently that KM-5 was considered a dry beach location. KM-2 and KM-6 were positioned on dry beach areas, while KM-4 and KM-7 were located on the berm. KM-3 was located on a wet beach area and had received tailings flow in the recent past; however, initial logging revealed that a seal had not been effected between the pipe and the tailings, hence no data are reported for this location.

Test holes UN-1 through UN-6 were implanted in October, 1977; UN-7 through UN-11, KM-1 and KM-2 were implanted in March, 1978; and all other emplacements were made in October, 1978.

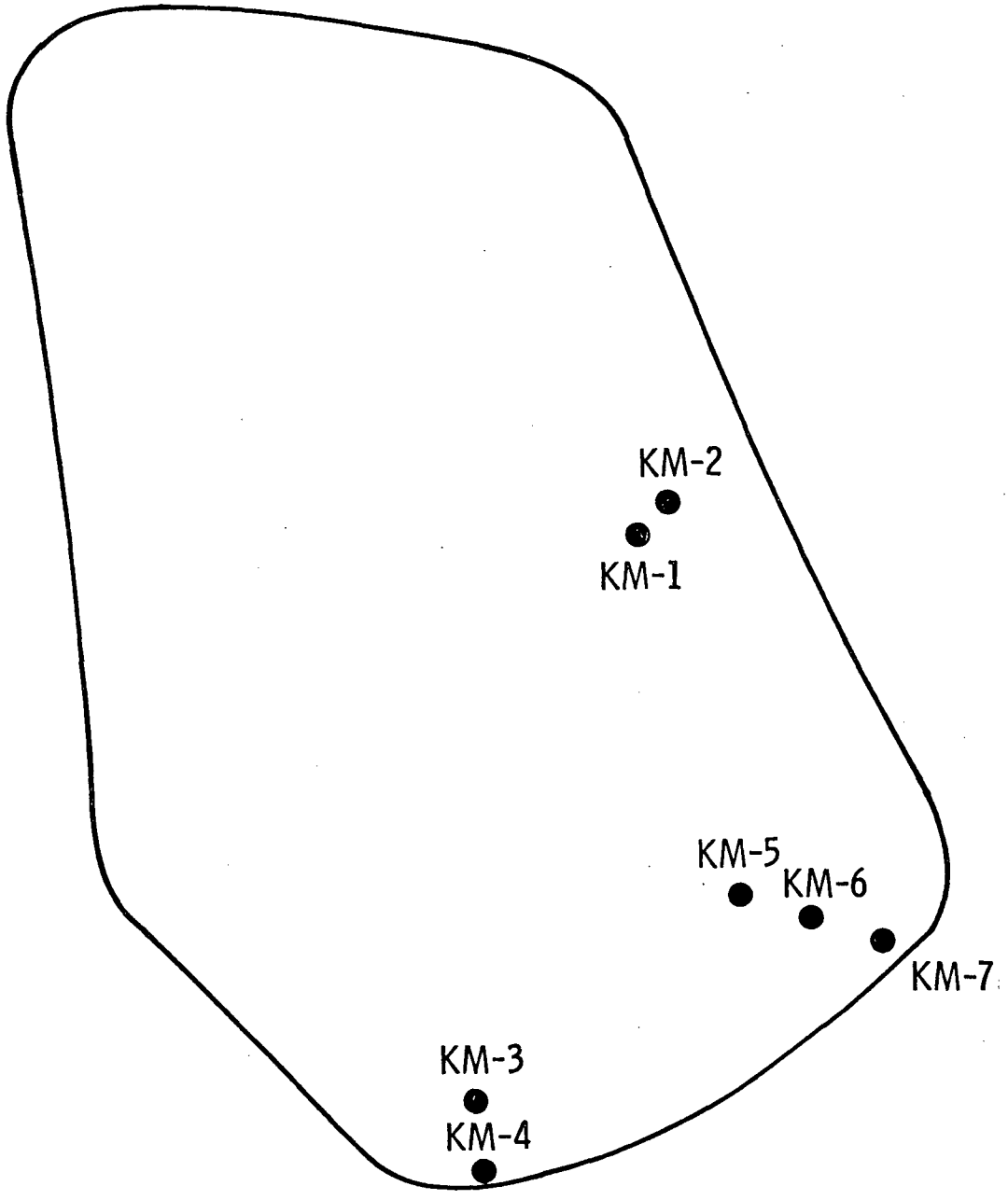

FIGURE 4. Test Locations at the Kerr-McGee Tailings Pile

In the course of predrilling the last series of holes at UN-12 and UN-13 and KM-4 through KM-7, random grab samples were taken for gravimetric determination of the moisture content of the tailings at different depths. Moisture contents determined by weight loss from a preweighed sample after air drying to constant weight at 110°C are given in Table I.

MEASUREMENT AND CALIBRATION

DOWNHOLE GAMMA-RAY SPECTROMETRY

Gamma-ray logging of the test holes was accomplished by sequentially lowering an intrinsic germanium detector to discrete depths and accumulating the resultant spectra for a sufficiently long period to obtain the desired counting statistics. The diode system, shown in two views in Figs. 5 and 6, consists of an intrinsic germanium diode (Princeton Gamma Tech) with an efficiency of 23% relative to a 7.62 x 7.62 cm NaI(Tl) crystal and a resolution of 1.96 keV at the 1333 keV ^{60}Co line. The dewar flask contained sufficient liquid nitrogen cryogen for about 9 hr of uninterrupted operation. A 20 mm thick lead shield, supported on top of the diode, limited the solid angle of interrogation to 2 π and accomplished two purposes. First, it improved resolution for determining concentration changes of radionuclides as a function of depth; and secondly, it limited the incident number of photons to a level that did not saturate the electronic processing system. The entire detector system was contained in a package fabricated from 14 cm O.D. PVC pipe which was fitted with an eye bolt for raising and lowering the unit. High voltage was supplied by a Harshaw Model NV-27 power supply. Signals from the diode were processed through a Model 1413 Canberra spectroscopy amplifier and analyzed and stored in the memory of a Tracor Northern Econ II 700 series analyzer. Data were retrieved using integrating circuitry within the analyzer to sum the events recorded in preselected channel groupings. Data were also recorded with a high speed printer to provide verification of the integrated output.

In the field, the distance from the top of the test hole casing to ground level was measured prior to gamma-ray logging to determine the degree of soil removal induced by wind erosion. The gamma probe was then positioned with the aid of a calibrated chain, and the gamma-ray spectrum at a discrete

TABLE 1

MOISTURE CONTENT OF URANIUM TAILINGS

Location	Depth cm	Moisture Wt %	Location	Depth cm	Moisture Wt %
KM-4	30	7.3	KM-6	24	12.3
	52	9.1		60	20.0
	57	5.6		114*	8.7
	78	7.6		124	11.6
	125	7.2		142	10.7
	160	8.1		196	9.9
	192	6.8		230	9.6
	222	6.4			
KM-5	28	18.6	KM-7	26	7.7
	63	21.6		80	7.3
	92	22.7		96	7.2
	116	19.0		121	7.4
	140*	7.7		138	7.9
	164	14.1		160	8.2
	190	10.2		206	7.9
UN-12	0	11.4	UN-13	10	2.3
	38	6.0		48	4.5
	100	15.8		76	6.0
	145	13.5		117	5.3
	215	9.5		163	10.1
				228	9.6

*Hard layer of clay-like material.

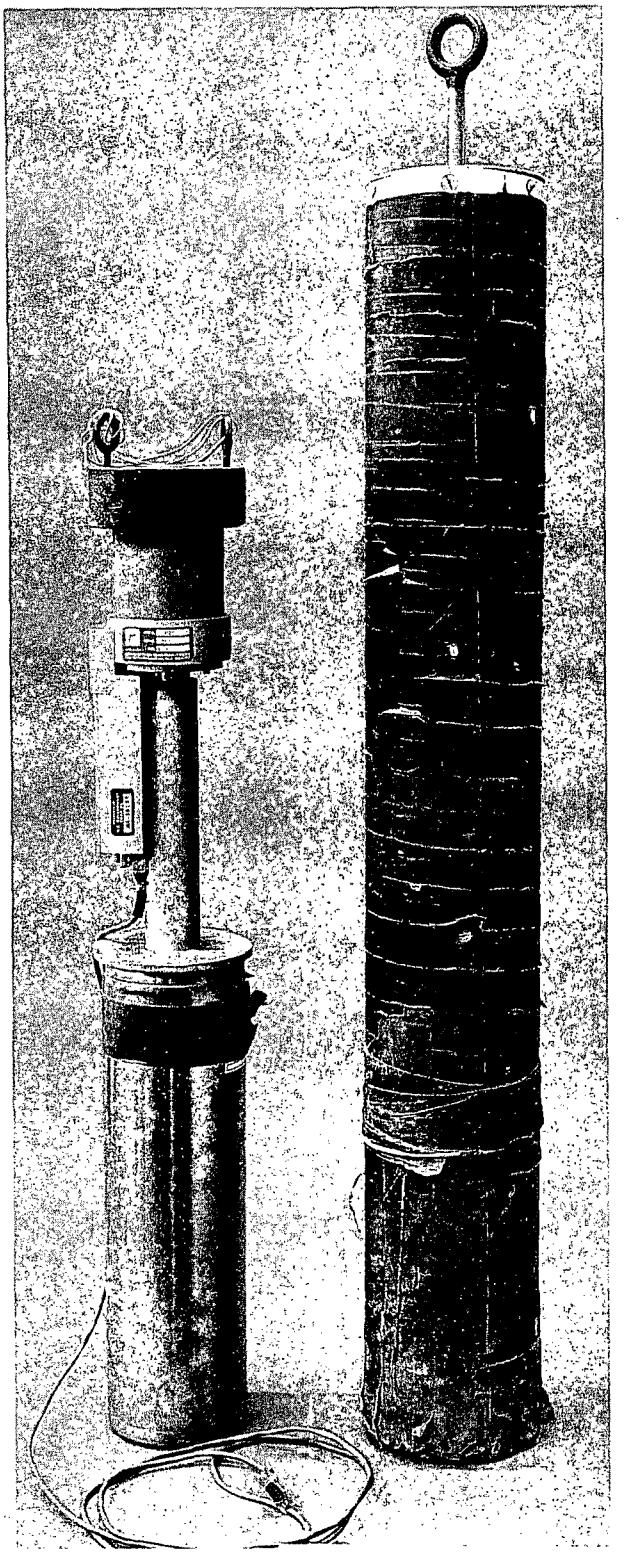

FIGURE 5. Gamma-ray Detector Probe--Assembled View

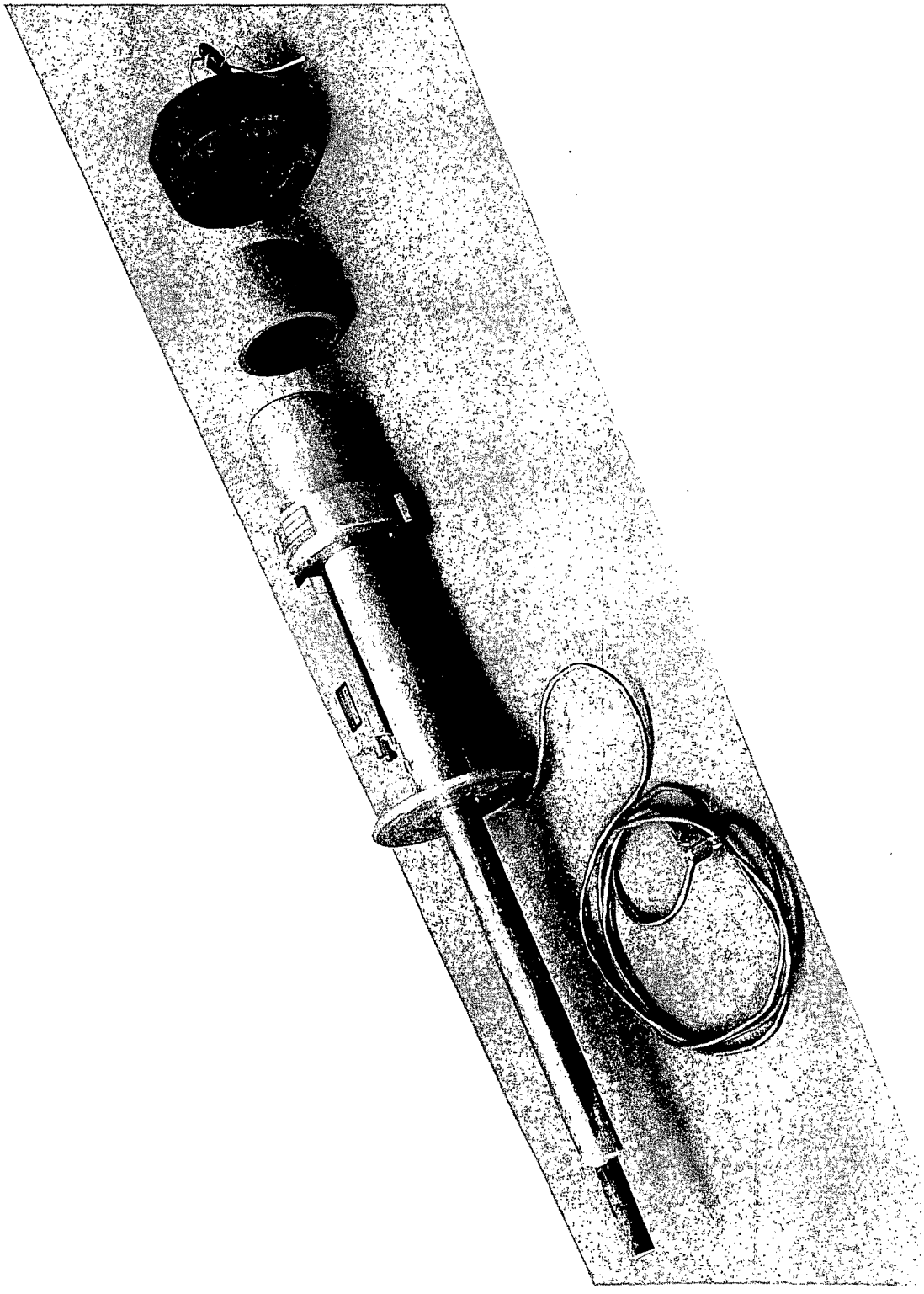

FIGURE 6. Gamma-ray Detector Probe--Expanded View

soil depth was accumulated. The diode was then repositioned and the process repeated until the hole was logged to the desired depth.

GAMMA PROBE CALIBRATION

It was calculated that 20 cm of tailings material would attenuate greater than 99% of the 186 keV and 352 keV photons from decay of ^{226}Ra and ^{214}Pb, respectively. Accordingly, a calibration facility was fabricated by axially installing a 15.2 cm diameter schedule 40 PVC pipe through the center of a 58 cm diameter steel drum. The drum annulus was then filled to a depth of 66 cm with homogenized uranium tailings of known radium concentration, containing less than 5% moisture by weight. The tailings were then sealed for 21 days to allow build-up of radon daughter concentrations to 98% of equilibrium. The shielded gamma probe was positioned within the annulus and gamma-ray spectra were obtained as a function of depth from the surface of the tailings material. The tailings were then saturated with water, the drum was resealed and radon and its daughters allowed to re-equilibrate, and another series of spectra were obtained as a function of depth. Within counting statistics, the counting rates obtained at specific depths in both wet and dry tailings were identical. From the net counting rates obtained at the 186 and 352 keV photopeaks of ^{226}Ra and ^{214}Pb, respectively, and the known concentrations of ^{226}Ra in the source, the calibration curves shown in Fig. 7 were generated. A 185 keV photopeak from decay of ^{235}U could cause interference in the measurement of radium, but the depletion of uranium in the tailings essentially negates this potential difficulty.

MEASUREMENT OF RADON FLUX BY ACTIVATED CHARCOAL ADSORPTION

The charcoal canister method of Countess[5] for radon collection and determination of radon flux from emanating surfaces has been widely accepted and utilized.[5,9] This method was reported to provide measurements of radon fluxes with an accuracy and precision of ±15%.[9] We used this collection technique with samplers shown in Fig. 8. Each sampler consisted of a 6.5 cm diameter PVC pipe and coupling that held 100 g of activated charcoal granules, supported on a filter-covered stainless steel screen and sealed on top with a rubber stopper. The sampler was twisted into the tailings surface to accumulate the radon escaping from the surface of the 40.7 cm^2 sampling

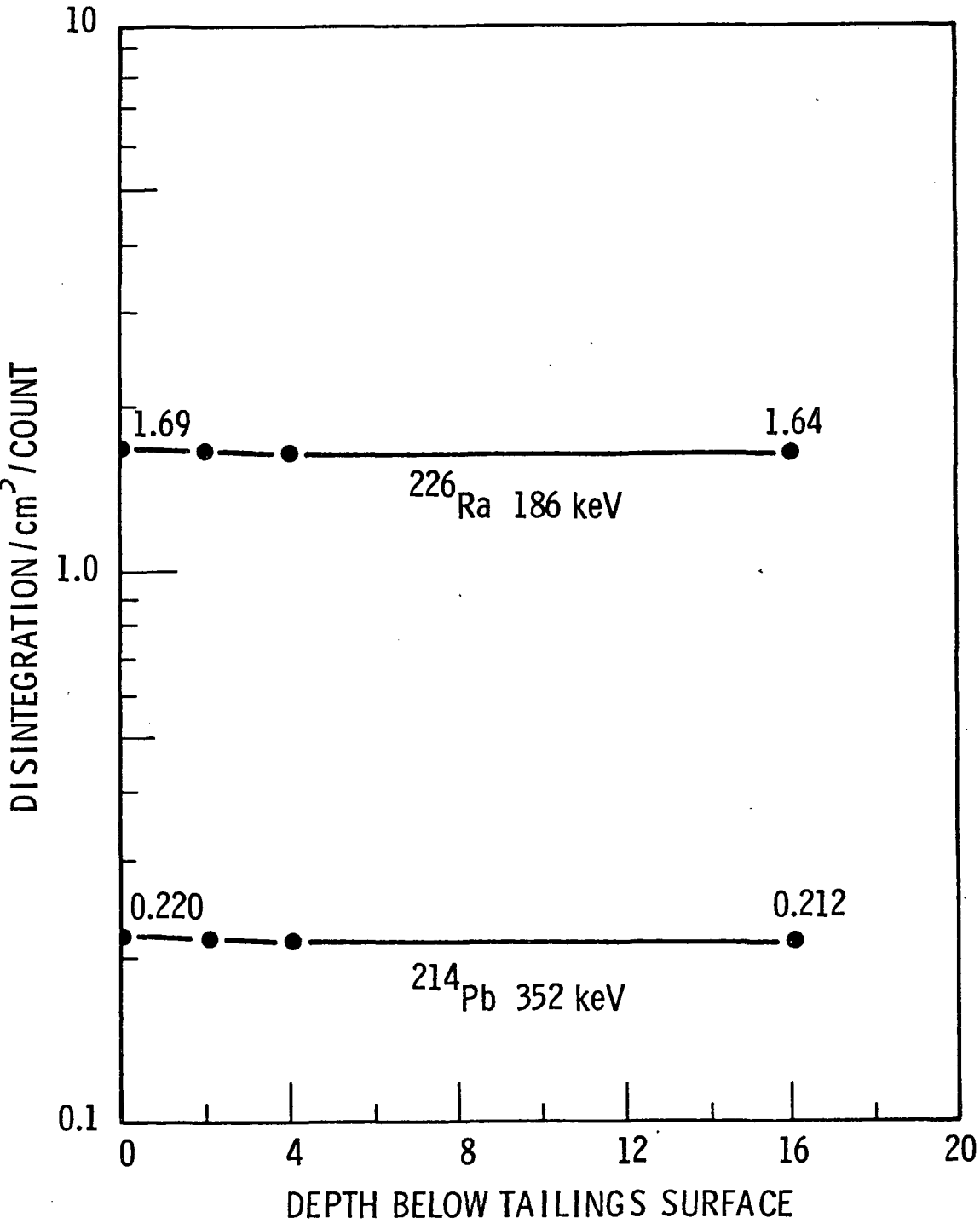

FIGURE 7. Detector Probe Calibration Curves

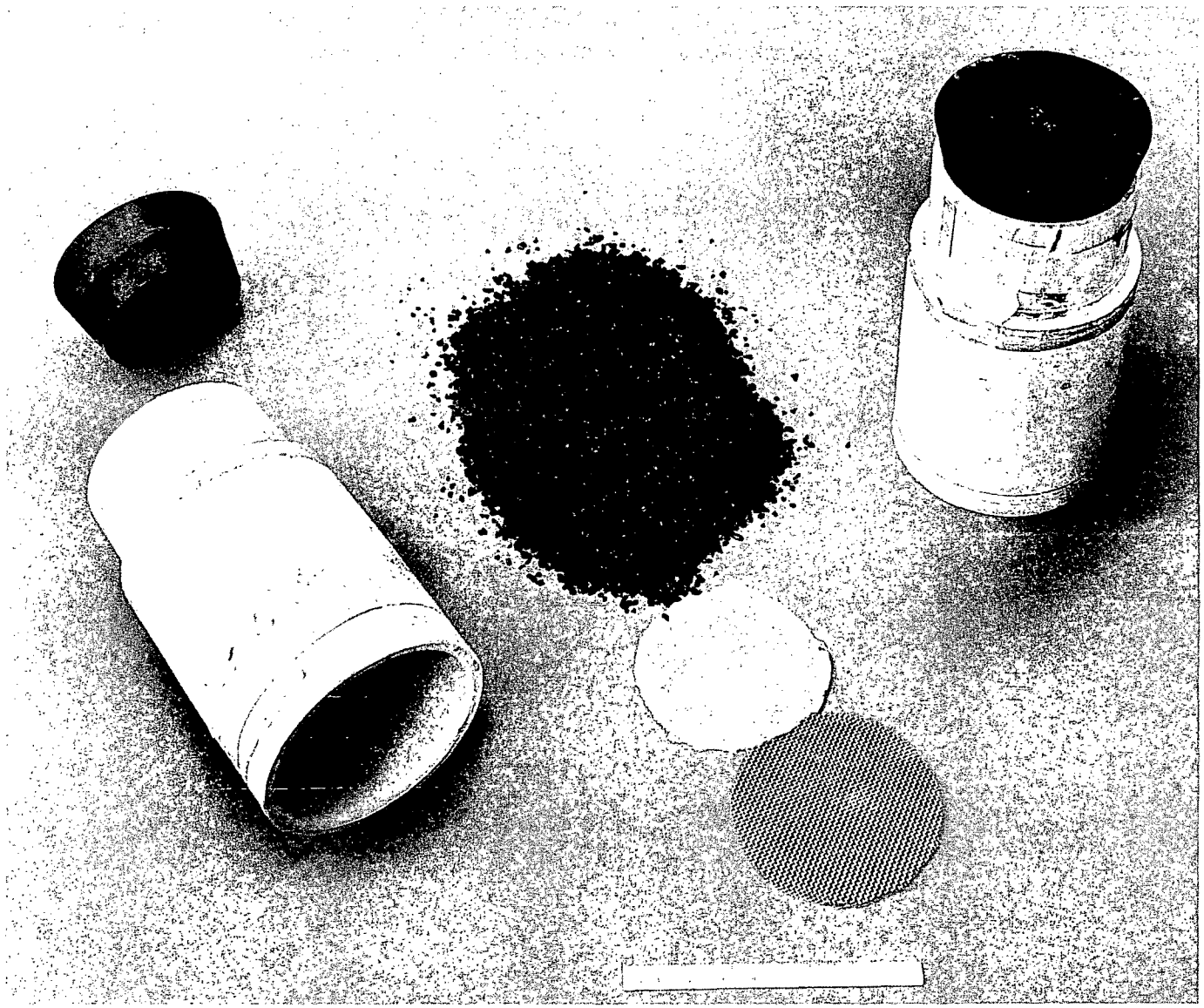

FIGURE 8. Charcoal Flux Canister

area. After exposure for a period ranging from several hours to several days, the canister was recovered and the charcoal was transferred to a 15 cm diameter x 2.5 cm thick plastic petri dish, sealed with plastic tape, and returned to the laboratory for analysis.

Sealing the charcoal in the petri dish accomplished two purposes: (1) elimination of radon loss from the sample; and (2) the surface charcoal, which retained most of the collected radon, was mixed with the remaining adsorbent, thus insuring an homogeneous sample and reproducible counting geometry.

Radon collected by the charcoal was determined by measurement of its ^{214}Pb and ^{214}Bi daughter concentrations by multidimensional gamma-ray spectrometry.[11] The spectrometer systems were calibrated by counting known standards contained in the same geometry as the charcoal samples to obtain the counter efficiency, or counts per disintegration, for the two radon daughters. Radon flux was calculated according to:

$$J_{(atoms/cm^2 \cdot sec)} = \frac{C}{(e^{-\lambda t_2})(1 - e^{-\lambda t_1}) E \cdot A}$$

where: C = net counts/second
λ = radon decay constant in $hours^{-1}$
t_1 = duration of canister exposure (hours)
t_2 = time lapse between end of sampling and start of counting (hours)
E = counter efficiency (counts/disintegration)
A = area of canister exposure (cm^2)

To convert flux values from $atoms/cm^2 \cdot sec$ to $Ci/cm^2 \cdot sec$, multiply by $\lambda(min^{-1})/2.22 \times 10^{12}$ d/m/Ci or 5.67×10^{-17}.

RADON DIFFUSION AND CURRENT MODELS

Two different methods were developed to calculate the radon current through soil. The first method assumes that the radon diffusion coefficient is constant throughout the depth of the hole and that a fixed proportion of the radon produced in the tailings escapes to the interstitial volume and diffuses through the soil. This method first calculates the diffusion coefficient and the proportion of diffusable radon, and these

quantities are then used to calculate the radon current. The second method uses a steady state mass balance equation to calculate the radon current. Both methods are capable of dealing with a nonuniform radium source. In fact, these two methods were developed for the present problem because existing diffusion models that assumed a homogeneous radium source could not be applied to the conditions of vertically nonuniform radium distributions that were encountered in tailings piles.

FIRST METHOD: THE DIFFUSION MODEL

Let C(z) and S(z) represent the true radon and radium decay rates at depth z; both values are defined in the same units, disintegrations/sec·cm^3. The z coordinate is positioned so that the positive axis points downward. Atom concentrations can be calculated, but because the formulae involving the disintegration rate distribution curves are slightly simpler than the atom concentration curves, the problem will be formulated in terms of the disintegration rate curves.

This model assumes that a constant proportion, α, of all the radon formed is free to diffuse in the soil, and the remainder, $1-\alpha$, is bound in the soil particles. Let $C_B(z)$ represent the bound radon at depth z and let $C_F(z)$ represent the free radon. The bound radon must satisfy the equation:

$$C_B(z) = (1-\alpha)\ S(z) \tag{1}$$

while the free radon must satisfy the following differential equation:

$$C_F(z) - \frac{1}{K^2}\ \frac{d^2}{dz^2}\ C_F(z) = \alpha\ S(z) \tag{2}$$

where $K = \sqrt{\frac{\lambda}{D}}$

λ = radon decay constant in sec^{-1}

D = diffusion coefficient cm^2/sec

This value for D accounts for the porosity and permeability of the tailings material at the time and site of measurement. As such, it is a measure of the rate of diffusion through the bulk medium and not just the interstitial volume of the medium. A detailed discussion of this difference

is given by Culot, et al.[11] and should be considered before use of our values of D in other solutions of the diffusion equation.

The above equation does not uniquely specify the relationship between $C_F(z)$ and $S(z)$; two boundary conditions must be imposed to accomplish this. If the diffusion rate of radon in soil is much lower than diffusion in air, then the concentration of free radon at the soil surface should be nearly zero. A reasonable boundary condition at $z = 0$ would then be:

$$C_F(0) = 0 \tag{3}$$

If the radium curve, $S(z)$, is relatively flat at the bottom of the hole, one would expect little or no radon diffusion to occur at this point, and the current should be approximately 0 at the bottom of the hole. Thus,

$$-\frac{1}{K^2}\ \frac{d}{dz}\ C_F(T) \cong 0 \text{ [or equivalent to } C'_F(T) \cong 0] \tag{4}$$

where T is the depth at the bottom of the hole

$-\frac{1}{K^2}\frac{d}{dz}\ (C_F)$ represents the current at z.

Once $C_B(z)$ and $C_F(z)$ are determined, they can be summed together to obtain $C(z)$:

$$C(z) = C_B(z) + C_F(z). \tag{5}$$

Equations (1) through (5) determine the relationship between $C(z)$ and $S(z)$. Notice that this relationship depends on two quantities, α and K. If so desired, the relationships described in the above equation could be expressed in terms of an integral equation. If the true curves $C(z)$ and $S(z)$ were available, one could use the preceding formula directly to determine the correct values for α and K. However, any procedure used to determine these values must contend with the discrete nature of the data and also with the fact that the data contain experimental error. Regression seems to be the most reasonable technique for dealing with these problems. The general strategy that will be employed in the regression approach is to assume the function $S(z)$ has a shape that relies on some unknown parameters $\underset{\sim}{\beta} = (\beta_0, \beta_1, .. \beta_m)$. We need not specify the exact relationship between S and $\underset{\sim}{\beta}$. It is sufficient to designate this relationship by the notation

$$S(z:\underset{\sim}{\beta})$$

The expression for $S(z:\underset{\sim}{\beta})$ can be inserted into formulae (1) through (5), and an explicit solution for C(z) can then be found. This expression, C(z), will also depend on the parameters $\underset{\sim}{\beta}$ and, additionally, on the parameters α and K. We emphasize this relationship by writing:

$$C(z:\underset{\sim}{\beta},\alpha,K)$$

Estimates for the parameters $\underset{\sim}{\beta}$, α, and K can be obtained by regressing the above functions on the data. Because of the nature of the expression $C(z:\underset{\sim}{\beta},\alpha,K)$, the regression will be nonlinear. It is also important to note that the regression can be made to make use of certain important information the measurement procedure produces.

The measurement procedure provides us with enough information to allow variance estimates of each decay-rate measurement to be calculated. Each decay-rate measurement is constructed by subtracting a background count from the gross count accumulated in the photopeak energy region, dividing by the accumulation time, and finally multiplying by a calibration factor. Hence, the formula for calculating a decay-rate is:

$$\text{decay-rate} = \frac{F\ (G - B)}{T} \tag{6}$$

where: F is the calibration factor;
T is the time of accumulation;
G is the gross count;
B is the background count.

The above formula allows us to calculate the variance of the decay-rate in terms of the variances of G and B:

$$\text{Var (decay rate)} = \frac{F^2}{T^2}\,[\text{Var (G)} + \text{Var (B)}] \tag{7}$$

Since G and B have Poisson distributions, estimates for their variance are simply G and B, respectively. Thus an estimate for the variance of the decay-rate measurement is:

$$\text{Var (decay rate)} = \frac{F^2}{T^2}\,(G + B) \tag{8}$$

These variance estimates can be used to construct weighting factors for the regression to allow data points with low variability to be weighted more heavily than those with high variability.

The weighted, nonlinear regression can be mathematically described as a procedure that minimizes the following sum of squares:

$$SSE(\underset{\sim}{\beta},\alpha,K) = \sum_{j=1}^{N} w_{cj}[C_j - C(z_j:\underset{\sim}{\beta},\alpha,K]^2 + \sum_{j=1}^{N} w_{sj}[S_j - S(z_j:\underset{\sim}{\beta})]^2 \qquad (9)$$

where: C_j = measured radon decay rate at depth z_j,
S_j = measured radium decay rate at depth z_j,
N = number of measurements taken,
w_{cj} = 1/(variance of measurement C_j),
w_{sj} = 1/(variance of measurement S_j).

When the data are regressed on the decay rate functions, the values that minimize $SSE(\underset{\sim}{\beta},\alpha,K)$ are the best estimates for $\underset{\sim}{\beta}$, α, and K. Figure 9 provides an illustration of this regression procedure.

Selection of a Form for $S(z:\underset{\sim}{\beta})$

It is desirable to select an expression for $S(z:\underset{\sim}{\beta})$ that will:

1. Approximate an arbitrary radium curve well; and

2. Produce an expression for $C(z:\underset{\sim}{\beta},\alpha,K)$ that is mathematically tractable.

With these two objectives in mind, it seemed best to choose the formulation:

$$S(z:\underset{\sim}{\beta}) = \sum_{j=1}^{M} \underset{\sim}{\beta}_j \cos(\omega_j z) \qquad (10)$$

where: $\omega_j = \frac{\pi}{T}(j-1)$

T = maximum depth at which a measurement was taken.

This trigonometric series will approximate any "smooth" function well in the interval 0 to T, if enough terms are included. The expression presented above can be substituted into equations (1) to (5) with the result:

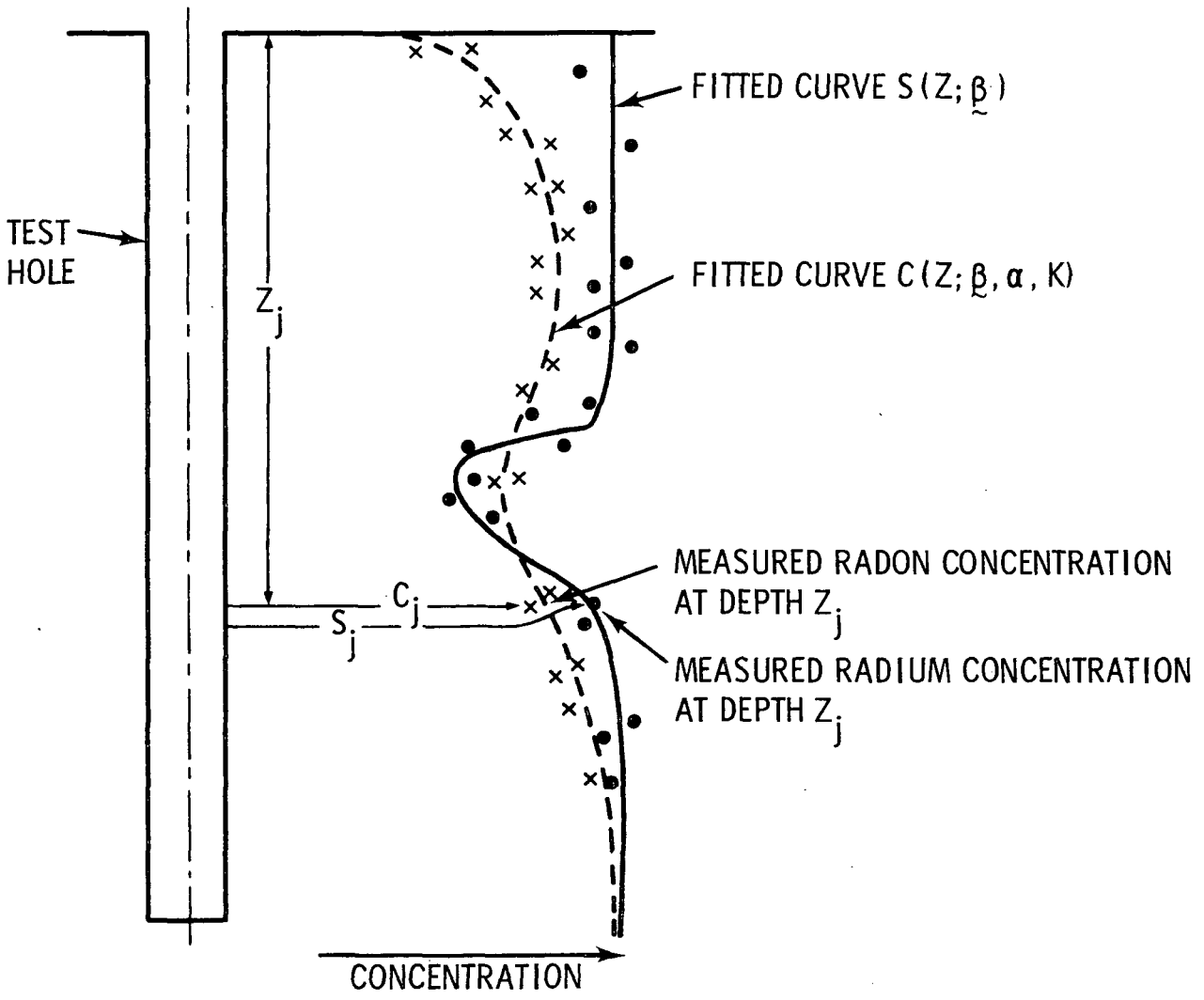

FIGURE 9. Graphic View of the Regression Procedure

$$C(z:\underset{\sim}{\beta},\alpha,K) = \sum_{j=1}^{M} \beta_j \left[\frac{\alpha K^2}{K^2 + \omega_j^2} U_j(z) + (1-\alpha) \cos(\omega_j z) \right] + \gamma K \sinh(Kz) \quad (11)$$

where: $U_j(z) = [\cos(\omega_j z) - e^{-Kz}]$,

$$\text{and} \quad \gamma = -\left[\sum_{j=1}^{M} \beta_j \frac{\alpha K}{K^2 + \omega_j^2} \right] \frac{e^{-KT}}{\cosh(KT)} \quad (12)$$

It is fairly easy to verify that (10) and (11) satisfy equations (1) through (5) by simply substituting these expressions back into the equations. The term $\gamma K \sinh(Kz)$ has been introduced into equation (11) to make C satisfy the second boundary condition (4). Equation (12) gives γ the proper magnitude to make the current zero at $z = T$. However, if T is large, the constant will be extremely small and the term $\gamma K \sinh(Kz)$ will be negligible. This fact can be used to simplify (11) slightly. The modified equation

$$C(z:\underset{\sim}{\beta},\alpha,K) = \sum \beta_j \left[\frac{\alpha K^2}{K^2 + \omega_j^2} U_j(z) + (1-\alpha) \cos(\omega_j z) \right] \quad (13)$$

will exactly satisfy equations (1), (2), (3), and (5), but will only approximately satisfy (4). Because of its greater simplicity, equation (13) was used to model the radon curves instead of equation (11).

Calculation of the Current J(z) for the Diffusion Model

Once the parameters $\underset{\sim}{\beta}$, α, K have been determined by regression, it is an easy task to calculate the radon current which is defined by the formula:

$$J(z) = -\frac{1}{K^2} \frac{d}{dz} C_F(z) \quad (14)$$

Since

$$C_F(z) = \sum_{j=1}^{M} \beta_j \frac{(\alpha)K^2}{K^2 + \omega_j^2} U_j(z) \quad (15)$$

we find that J(z) must have the form:

$$J(z) = \alpha \sum_{j=1}^{M} \frac{\beta_j}{K^2 + \omega j^2} \left[\omega_j \sin(\omega_j z) - Ke^{-Kz}\right]. \qquad (16)$$

Substituting the regression estimates for β, α, and K into the above formula will provide an estimate of the radon current curve.

POOLING THE DATA

As discussed earlier, each hole was measured several times on different dates. As long as the tailings were not physically disturbed, one would expect the radium concentration at a specific depth to remain the same, which suggests that all radium measurements for a specific location can be profitably pooled together to help one obtain a more accurate description of the radium concentration. Pooling radium measurements helps to rectify a basic weakness in the measurement process. Radium decay rates were measured with approximately 1/10 the precision of radon decay rates; thus, pooling the radium data helps to add definition to the curve we know the least about.

Pooling would modify the regression equations presented in the previous sections in a straightforward way, if it weren't for one annoying complication. In some instances, wind erosion altered the location of the soil surface, in one case by as much as 37 cm, which must be accounted for in the pooling calculations.

Suppose measurements at a certain hole have been collected on dates i = 1,2,3..p and suppose the location of the soil surface on each of these different dates is given by z_{i0}, i = 1,2,3..p. Denote the measurements taken on date i by:

C_{ij} for the radon decay rate measured at depth z_{ij}.

S_{ij} for the radium decay rate measured at depth z_{ij}.

The formula describing the radium decay rate is the same as before:

$$S(z) = \sum_{j=1}^{M} \beta_j \cos(\omega_j z) \qquad (17)$$

but the formula describing the radon decay rate is:

$$C_i(z) = \sum_{j=1}^{M} \beta_j \left[\frac{(\alpha_i) K_i^2}{K_i^2 + \omega_j^2} \; U_{ij}(z) + (1-\alpha_i) \cos(\omega_j z) \right] \qquad (18)$$

$$\text{where } U_{ij}(z) = \cos(\omega_j z) - \cos(\omega_j z_{io}) \; e^{-K_i (z - z_{io})}$$

The regression procedure now attempts to fit the curves $S(z)$, $C_1(z)$, $C_2(z)$ ...$C_p(z)$ to all the data simultaneously. The regression procedure chooses values for β, α, and K that minimize the following sum of squares:

$$SSE(\underset{\sim}{\beta},\alpha,K) = \sum_{i=1}^{P} \left[\sum_{j=i}^{N_i} w_{sij} \left(S_{ij} - S(z_{ij}) \right)^2 + \sum_{j=1}^{N_i} w_{Cij} \left(C_{ij} - C_i(z_{ij}) \right)^2 \right] \qquad (19)$$

In light of this discussion, Equation (19) instead of Equation (9) was employed to ascertain the best values for $\underset{\sim}{\beta}$, α, and K from the data.

SECOND METHOD: MASS CONSERVATION MODEL

This model rests on the assumption that, when in steady state, the number of radon atoms leaving a system must balance with those entering it. In this case, the system of interest is a 1-cm square column of soil beginning at depth z and extending down to depth T.

Radon atoms enter and leave this system through the 1-cm square faces of the column at depth z and depth T. The total number of such atoms to enter the system in one second is:

$$J(z) - J(T), \qquad (20)$$

where $J(z)$ and $J(T)$ are the radon currents at depths z and T. If expression (20) is negative, it represents a loss of radon from the system.

Radon atoms also enter this system from the decay of radium atoms. The number of radon atoms that are produced in one second from this source is:

$$\int_z^T S(t)dt \qquad (21)$$

Finally, radon atoms leave the system by decay; the number of radon atoms leaving the system in one second by this mechanism is:

$$\int_z^T C(t)dt \tag{22}$$

Expressions (20) and (21) must balance with (22), hence:

$$J(z) = \int_z^T C(t)dt - \int_z^T S(t)dt + J(T). \tag{23}$$

In addition, if the point T has been chosen so that no radon travels across the bottom of the column, then

$$J(z) = \int_z^T C(t)dt - \int_z^T S(t)dt. \tag{24}$$

If one had the complete decay rate curves C(z), it would be a simple matter to calculate J(z). However, the data provide us with only a few points on each of these curves, mixed with experimental error. Regression can again be used to deal with these problems.

We again choose to model the C(z) and S(z) curves using a trigonometric series of the form:

$$\left.\begin{matrix} C(z) \\ S(z) \end{matrix}\right] = \sum_{j=0}^{M} B_j \cos(\omega_j z) \tag{25}$$

where B_j are parameters to be determined by regression, and

$$\omega_j = \frac{\pi K}{T}$$

This not only gives us an estimate of J(z) by Equation (24), but also provides error bounds for this estimate. By including enough terms, an expression of the above form can be made to fit any "smooth" function in the interval between 0 and T arbitrarily closely. If the integrals in (24) are evaluated, we obtain:

$$\int_z^T \begin{bmatrix} C(z) \\ S(z) \end{bmatrix} dz = \int_z^T \sum_{j=0}^{M} B_j \cos(\omega_j z) dz = B_0(T-z) - \sum_{j=1}^{M} \frac{B_j}{\omega_j} \sin(\omega_j z) \qquad (26)$$

Hence, the formula for current is:

$$J(z) = (B_{co} - B_{so})(T-z) + \sum_{j=1}^{M} (B_{sj} - B_{cj}) \frac{\sin(\omega_j z)}{\omega_j} \qquad (27)$$

where: B_{cj} are parameters from the regression of (25) on the radon data.
B_{sj} are parameters from the regression of (25) on the radium data.

RADIONUCLIDE CONCENTRATIONS AND DETERMINATION OF DIFFUSION PARAMETERS

The first detailed measurements of radionuclide concentrations in test holes at the UN-HP site were made in December 1977. Additional test holes were implanted in March and October 1978, at which times most holes were re-logged, if accessible. A final series of field measurements were conducted during May 1979 in which intensive measurements were made at four locations of the UN-HP site and three at the Kerr-McGee plant. The concentrations of ^{226}Ra and ^{214}Pb determined from these spectra are given in Appendix 1. The 186 keV photopeak, used for determination of radium, was located on the Compton scatter slope of the spectrum. Its magnitude was evaluated by incremental difference between two rather large numbers resulting in a relatively high degree of uncertainty, and the pooling procedure previously described was applied to more accurately evaluate the vertical radium distribution at the individual sampling locations.

As detailed in the preceding section, values for the diffusion coefficient and radon emanation factor were determined by regressing the decay rate curves on the data. Examples of the fits obtained with the pooling procedure for the radium data are shown in Fig. 10, and comparison of the measured and predicted radon curves for measurements at UN-1B on 5/13/79 is given in Fig. 11.

The diffusion coefficients as calculated are "average" values that provide the best fit of the radium and radon concentrations present within a given depth. We recognize that assumption of a uniform diffusion coefficient is invalid in the true sense, because diffusion at a specific depth is going to depend on such factors as the conditions of soil moisture and porosity existent at that depth. Most of the radon exhaled from the tailings surface is derived from the upper soil layer, although the quantity and rate is influenced by driving forces induced at greater depths. For this reason, it was decided to evaluate diffusion parameters for both the top meter of tailings and the maximum depth to which each hole was logged. If the calculated diffusion coefficients were the same at both depth intervals, it seems reasonable to assume that the diffusion model should provide reliable estimates of both the rate of radon diffusion and the exhalation of radon from the tailings surface. If the calculated diffusion constants varied significantly from the two data sets, then the magnitude of error in assuming uniform diffusion with depth would be suggested. In the majority of cases presented in Table 2 there was excellent agreement for the values calculated for D and α for maximum depth and those calculated for the top meter of tailings. Somewhat higher values were obtained at full depth in holes 10 and 1B, although even in these cases values were in agreement within 2σ error limits. Thus it appears that although the conditions can exist that influence radon diffusion at different depths, the magnitude of these influences is small enough to be ignored within the diffusion layer of the tailings pile. Indeed, some of the apparent differences in D and α were offsetting, that is, α would increase while D decreased, most probably as a result of the fitting procedures employed in calculations. A salient point to remember is that the radon flux is directly proportional to the emanation coefficient and varies as the square root of the diffusion coefficient. Thus an increase in D of a factor of four will double the calculated radon flux at a constant emanation coefficient.

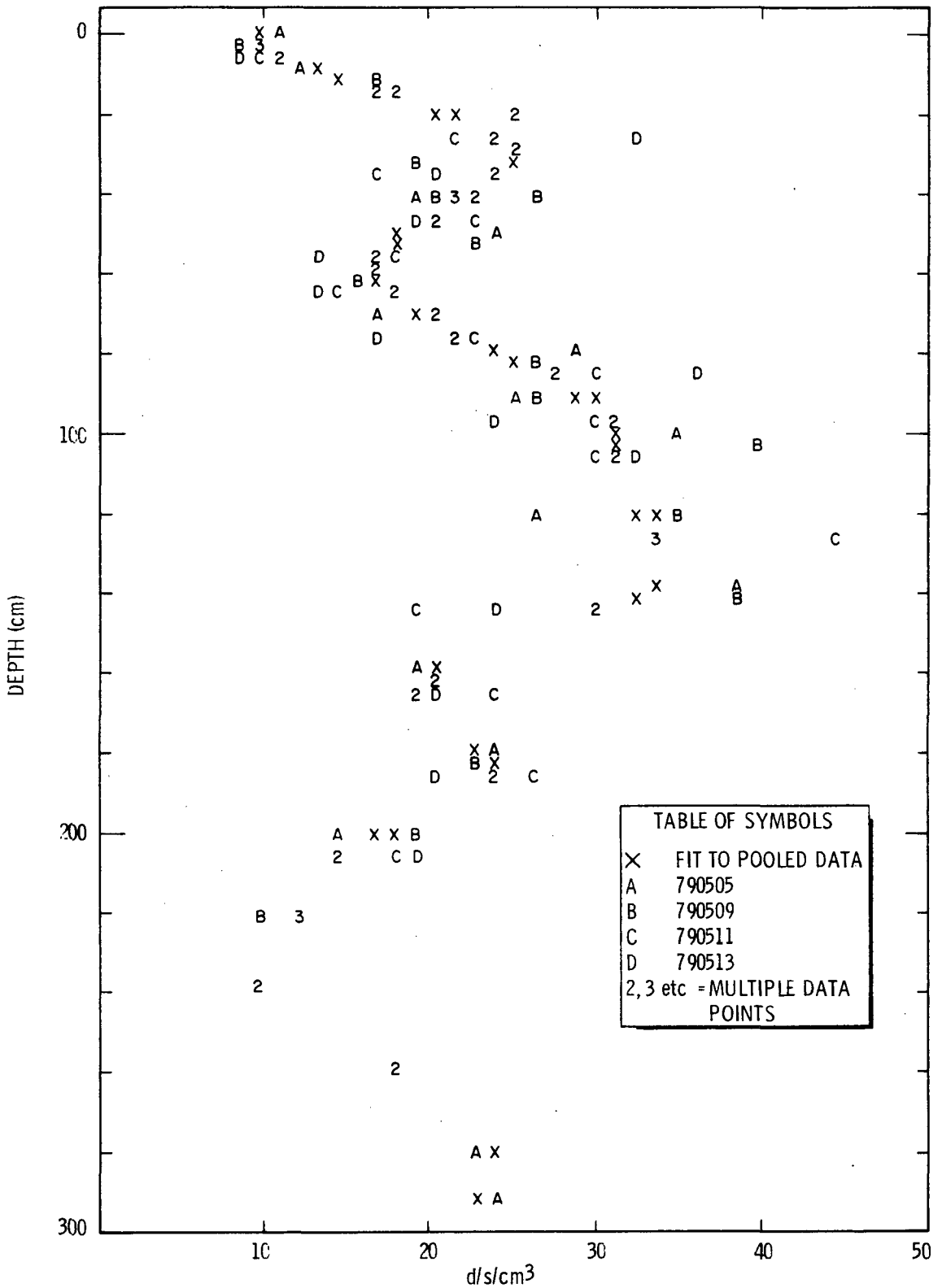

FIGURE 10. Measured and Pooled Radium Data, UN-1B

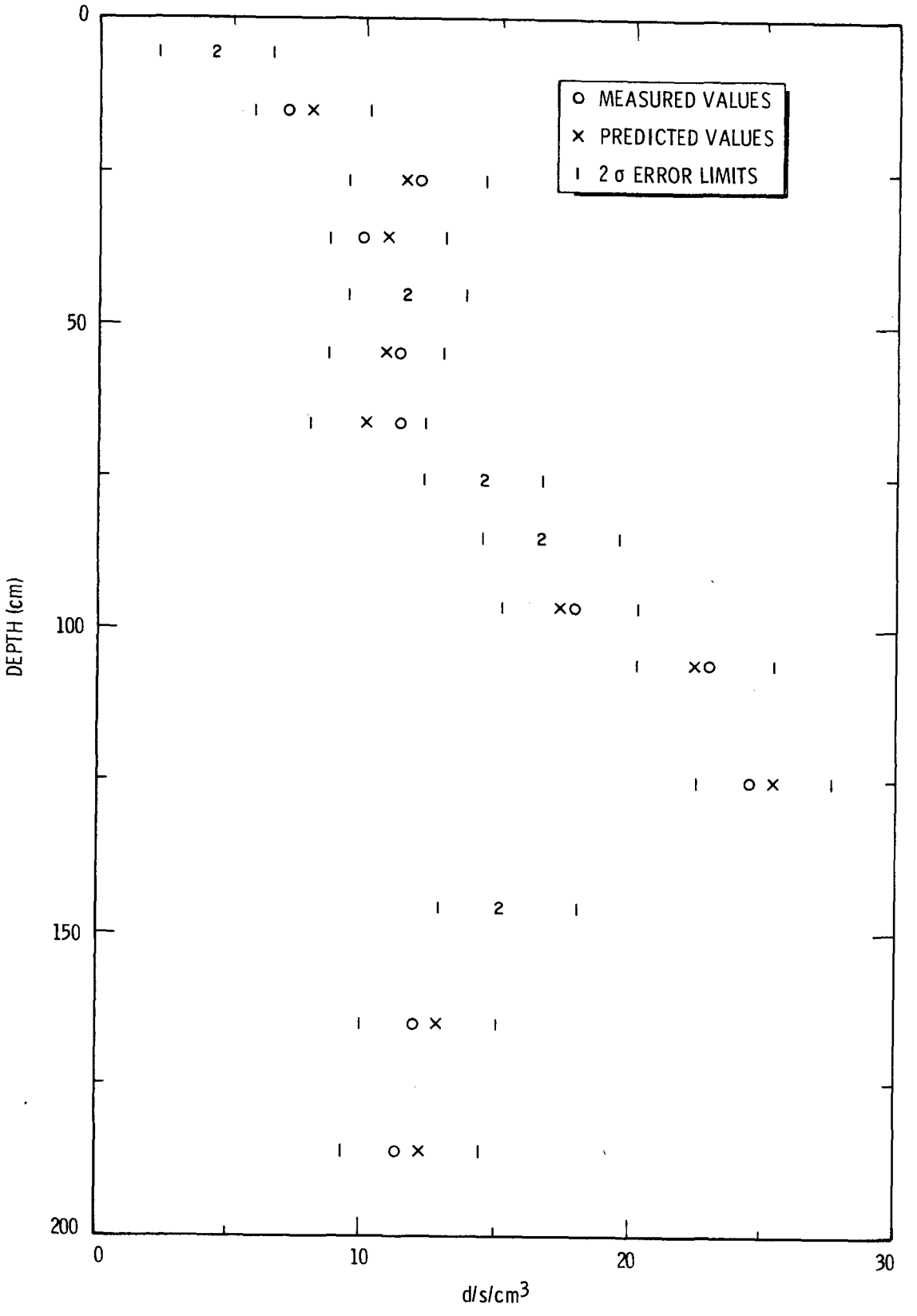

FIGURE 11. RADON-222 CONCENTRATIONS, UN-1B ON 5/13/79

TABLE 2

CALCULATED RADON DIFFUSION AND EMANATION COEFFICIENTS

Sample Location	Tailings Area(1)	Date	100 cm α	100 cm D (cm^2/sec)	Z(T)	Maximum Depth α	Maximum Depth D (cm^2/sec)
UN-1	DB	12/6/77	0.60±.05(2)	0.0039±.0010(2)	(3)		
		3/20/78	0.46±.06	0.0032±.0013			
UN-1B	DB	5/5/79	0.42±.05	0.0054±.0025	190	0.38±.05	0.0091±.0038
		5/9/79	0.46±.05	0.0074±.0031		0.39±.05	0.0103±.0043
		5/11/79	0.48±.05	0.0065±.0020		0.33±.05	0.0190±.0095
		5/13/79	0.47±.06	0.0050±.0021		0.35±.05	0.0127±.0059
UN-2	DB	12/7/77	0.40±.05	0.0022±.0013	200	0.40±.05	0.0022±.0012
		3/20/78	0.43±.05	0.0020±.0011		0.42±.05	0.0018±.0010
UN-3	WB	12/7/77	(5)				
		3/20/78	0.05±.03	0.68 ±.15	200	0.05±.04	0.0016±.0061
UN-4	S	12/7/77	(5)			(6)	(6)
		3/21/78	(6)	(6)		(6)	(6)
UN-5	DB	12/8/77	0.54±.04	0.0005±.0020	190	0.56±.05	0.0005±.0002
		3/23/78	0.52±.03	0.0032±.0010		0.54±.02	0.0027±.0008
UN-6	B	12/8/77	0.44±.06	0.0124±.0090	(3)		
		3/22/78	0.43±.06	0.0041±.003			
UN-7	WB	12/8/77	0.49±.10	0.0009±.0006	200	0.39±.03	0.064 ±.018
		3/22/78	0.30±.06	0.0032±.0029		0.34±.06	0.0008±.0005
UN-8	WB	12/3/77	(5)				
		3/21/78	0.30±.03	0.00014±.00009	195	0.27±.03	0.00002±.00001
UN-9	B	12/7/77	0.44±.06	0.015±.010	(3)		
		3/21/78	0.46±.05	0.020±.016			
UN-9B	B	5/5/79	0.37±.07	0.033±.034	200	0.40±.07	0.019±.012
		5/9/79	0.35±.07	0.013±.015		0.36±.06	0.014±.009
		5/11/79	0.36±.07	0.016±.018		0.35±.06	0.022±.016
		5/13/79	0.36±.07	0.016±.019		0.36±.06	0.016±.010
		5/15/79	0.35±.10	0.023±.056		0.37±.07	0.017±.012
UN-10	WB	12/8/77	0.20±.10	0.0023±.0043	205	0.19±.08	.0029±.0046
		3/23/78	0.42±.07	0.0039±.0027		0.32±.05	.0244±.0133
UN-11	B	12/8/77	0.45±.09	0.0089±.0065	(3)		
		3/22/78	(4)				

TABLE 2 (continued)
CALCULATED RADON DIFFUSION AND EMANATION COEFFICIENTS

Sample Location	Tailings Area(1)	Date	100 cm			Maximum Depth	
			α	D (cm^2/sec)	X	α	D (cm^2/sec)
KM-1	WB	3/25/77	0.24±.07	0.00045±.00063	(3)		
KM-2	DB	3/25/77	0.15±.08	0.022 .061	114	0.19±.07	0.0095±.0110
KM-4	B	10/28/78	0.20±.03	0.135 ±.298	200	0.21±.03	0.039 ±.037
KM-5	WB	10/28/78	0.22±.02	0.010 ±.005	200	0.23±.03	0.0049±.0021
	DB	5/6/79	0.15±.03	0.0014±.0012		0.15±.03	0.0009±.0008
		5/8/79	0.17±.03	0.0026±.0021		0.16±.03	0.0019±.0013
		5/11/79	0.20±.03	0.0019±.0013		0.20±.03	0.0015±.0008
		5/12/79	0.19±.03	0.0020±.0014		0.20±.03	0.0013±.0008
		5/14/79	0.18±.03	0.0025±.003		0.18±.03	0.0015±.0010
		5/16/79	0.22±.03	0.0008±.0005		0.22±.03	0.0006±.0003
KM-6	DB	10/25/78	0.26±.03	0.0006±.0002	(4)		
		10/29/78	0.24±.03	0.0004±.0002			
		5/6/79	0.19±.03	0.0012±.0006			
		5/8/79	0.15±.03	0.0020±.0013			
		5/10/79	0.18±.02	0.0026±.0012			
		5/11/79	0.21±.03	0.0037±.0017			
		5/12/79	0.18±.03	0.0033±.0017			
		5/14/79	0.10±.03	0.016±.015			
KM-7	B	10/29/78	(4)		190	0.16±.05	0.0014±.0013
		5/6/79				0.11±.04	0.023±.026
		5/8/79				0.15±.04	0.011±.008
		5/10/79				0.08±.04	0.012±.018
		5/11/79				0.06±.03	0.036±.075
		5/12/79				0.09±.03	0.043±.067
		5/14/79				0.06±.03	0.008±.010
		5/16/79				0.09±.04	0.009±.013

1 B = berm, DB = dry beach, WB - wet beach, S = saturated
2 Error limits are the standard deviation of the estimate of the parameter
3 Maximum depth of hole 100 cm
4 Regression predicted negative D
5 Too few data points for analysis
6 Concentration gradients too small to calculate values for D and α

Let us first consider the overall ramifications of these data and then compare the diffusion coefficients in relation to the field conditions that existed at the time of measurement. This discussion will be based on the values of K and α obtained with depth limited to 100 cm, with the exceptions of UN-3 and KM-7 where a better fit was obtained by using data to the full depth of the hole.

In general, 40% to 50% of the radon produced in the alkaline leach tailings is diffusable, compared with about 20% for the acid leach tailings. This is believed to reflect differences in the degree of fineness to which the ore was milled in the two processes, the carbonate leach process requiring a more finely ground ore in order to efficiently contact and solubilize the uranium. Thus the surface-to-volume ratio of tailings from the carbonate leach mill is much higher than occurs in acid leach tailings, enhancing the probability of escape of radon atoms to the interstitial volume and hence its availability to migrate by diffusion. High concentrations of soil moisture reduce the amount of diffusing radon by presenting an additional barrier to diffusion and by dissolving free radon.[1] In test hole UN-4 where the tailings were saturated and covered with standing water, radon emanation and/or diffusion was so low that no radon gradient was measurable by the in-situ method. In wet beach areas, represented by holes UN-3, -7, -8, and -10, values of the emanation factor as low as 0.05 to 0.30 were determined. UN-5 was implanted at a location originally classed as dry beach; however, the diffusion coefficient of 5×10^{-4} cm^2/sec determined on December 8, 1977, is more aptly ascribed to wet beach conditions. In the following year, a value more representative of dry beach conditions was found. Diffusion coefficients determined at given locations both during individual sampling periods and between periods several months apart were remarkably consistent, in most cases within the experimental error. Different values of the emanation coefficient derived from some data obtained on different dates can be explained by changes in soil moisture content that occurred at these locations between samplings. Although soil moisture content and profile were not quantified, observed changes qualitatively respond to the conditions observed during sampling efforts, e.g., UN-8 and -10 had dried out between December 1977 and March 1978, while UN-3 and -7 appeared

to contain increased soil water. In general, calculated emanation coefficients for data gathered from the top meter were equal to or greater than the values derived from the profiles to additional depths. This may reflect the influence of a somewhat increased moisture content at depth in reducing the degree of radon escapement and is manifested in a reduction in the average fractional quantity of radon throughout the increased depth interval that is available for diffusion.

There were two instances of major data sets, KM-6 at maximum depth and KM-7 at 100 cm, in which the regression predicted negative diffusion coefficients and extremely low values for α. In the case of KM-6, a concentration peak in the radium depth profiles was present just below 100 cm, and a layer of compacted clay material was also found at this depth. A probable explanation would be that this clay layer formed a significant barrier to radon diffusion within the soil column and errors in parameter estimates resulted from trying to describe diffusion through this complex system by a single-phase analysis.

For comparative purposes, averages of all values for D and α are given in Table 3, in which data are grouped according to the general tailings area from which they were derived.

TABLE 3

AVERAGED RADON DIFFUSION AND EMANATION COEFFICIENTS

	Alkaline Leach Tailings		Acid Leach Tailings	
	α	D cm^2/sec	α	D cm^2/sec
Wet beach	0.36	0.0010	0.20	0.0027
Dry beach	0.43	0.0042	0.19	0.0037
Berm	0.40	0.015	0.12	0.017

It is easy to see from these data that the rate of radon diffusion is higher at the berms which are comprised of the coarsest tailings material and are also the driest portions of the tailings piles. Diffusion rates successively decrease in the dry and wet beach areas, and in the case of UN-4 were too low to be determined by the in-situ logging technique.

Again, roughly 40% of the radon production was available for diffusion in the carbonate leach tailings compared with 20% in the acid leach pile. In most instances, diffusion constants calculated from data extending to different depths were not greatly different. Thus, the basic presumption of diffusional uniformity made in the derivation of the diffusion equation is substantiated by the field data. Equally important is that good estimates of the diffusion parameters can be made from data collected to moderate depths (∿100 cm), which greatly simplifies implantation of test holes for subsequent field experiments.

RADON EXHALATION AT TEST LOCATIONS

Proof of the validity of the diffusion model is its accuracy in predicting the quantity of radon escaping the tailings surface. The flux of radon escaping the pile at the sampling locations was determined by three methods:

1. By Equation (16) of the diffusion model where surface flux is calculated from the measured radium distribution and the values for α and D determined by regression as described in the preceding section.

2. By the mass conservation model (Equation 27), which determines the difference in total concentrations of radon and radium under the curves developed from the measured data. This method would be absolute if radium and radon were measured to a depth at which they were in equilibrium, which is the case for many of the measurements that were made.

3. By collection and analysis of radon exhaled from a known surface area with a charcoal canister exposed for a known period of time.

Fluxes determined at the different sampling locations by these three methods are given in Table 4. The reported errors are basically those arising from counting statistics, and in the case of fluxes determined by charcoal adsorption were limited to less than ±5% with the concentrations encountered and counting times employed.

It must be emphasized that the fluxes determined by the model and mass balance both yield values that are predicated on losses of radon that have previously occurred, and as such integrate radon losses over time periods

TABLE 4

RADON FLUXES FROM ACTIVE URANIUM TAILINGS PILES

(atoms/cm^2·sec)

Location	Date	J Diffusion Model (100 cm)	J Mass Balance	J Charcoal
UN-1	12/6/77	290 ± 30	260 ± 30	--
	3/20/78	200 ± 40	170 ± 30	70
UN-1B	5/5/79	290 ± 60	370 ± 70	230
	5/9/79	380 ± 70	300 ± 80	80
	5/11/79	380 ± 70	460 ± 80	120
	5/13/79	330 ± 60	420 ± 70	120
UN-2	12/7/77	180 ± 50	210 ± 70	
	3/20/78	180 ± 40	180 ± 70	200
UN-3	3/20/78	35 ± 60[a]	10 ± 90	40
UN-5	12/8/77	240 ± 30	470 ± 90	
	3/23/78	420 ± 50	530 ± 90	50
UN-6	12/8/77	340 ± 110	240 ± 40	
	3/22/78	190 ± 60	170 ± 40	--
UN-7	12/8/77	110 ± 30	80 ± 40	
	3/22/78	120 ± 40	100 ± 40	130
UN-8	3/23/78	60 ± 20	(b)	100
UN-9	12/7/77	380 ± 100	230 ± 30	
	3/23/78	440 ± 150	200 ± 20	120
WN-9B	5/5/79	420 ± 160	280 ± 60	
	5/9/79	250 ± 110	210 ± 70	
	5/11/79	280 ± 130	240 ± 50	
	5/13/79	280 ± 140	230 ± 40	
	5/15/79	330 ± 320	240 ± 60	
UN-10	12/8/77	70 ± 50	40 ± 40	
	3/23/78	200 ± 50	260 ± 60	80
UN-11	12/8/77	290 ± 80	190 ± 30	
KM-1	3/25/78	60 ± 40	50 ± 60	
KM-2	3/25/78	340 ± 370	200 ± 90	

TABLE 4 (continued)
RADON FLUXES FROM ACTIVE URANIUM TAILINGS PILES (continued)

Location	Date	J Diffusion Model (100 cm)	J Mass Balance	J Charcoal
KM-4	10/28/78	460 ± 200[a]	370 ± 90	520
KM-5	5/6/79	110 ± 40	(b)	170
	5/8/79	160 ± 50	30 ± 60	290
	5/11/79	170 ± 40	110 ± 60	470
	5/12/79	160 ± 40	110 ± 60	260
	5/14/79	160 ± 40	100 ± 60	358
	5/16/79	130 ± 30	50 ± 50	260
KM-6	10/28/78	150 ± 30	110 ± 40	410
	10/29/78	110 ± 30	80 ± 40	390
	5/6/79	150 ± 30	220 ± 60	460
	5/8/79	150 ± 40	290 ± 60	380
	5/10/79	220 ± 40	100 ± 60	540
	5/11/79	280 ± 50	140 ± 70	280
	5/12/79	250 ± 50	350 ± 70	210
	5/14/79	280 ± 90	110 ± 60	230
KM-7[c]	10/29/78	70 ± 30	100 ± 30	140
	5/6/79	210 ± 90	150 ± 30	150
	5/8/79	190 ± 60	160 ± 30	--
	5/10/79	100 ± 60	90 ± 30	210
	5/11/79	150 ± 60	100 ± 30	220
	5/12/79	220 ± 150	130 ± 30	220
	5/14/79	70 ± 40	90 ± 30	180
	5/16/79	100 ± 60	110 ± 30	210

(a) Calculated for maximum depth
(b) Radon inventory exceeded production
(c) Based on maximum depth

of many days preceding the measurement. Fluxes determined by charcoal adsorption are in essence point measurements of the exhalation that occurred during the sampling intervals.

Fluxes calculated by the diffusion model averaged 20% higher than those obtained by mass balance, which is considered an excellent agreement for such a diverse data set. The mass balance calculation was indeed predicted to be low, as in many instances the measurements were not made to sufficient depths to insure radium-radon equilibrium. Thus, in these instances the radon depletion layer extended below the intergration interval and a fraction of the radon deficiency was unaccounted in the cumulative inventory calculations. This favorable comparison substantiates the validity of the diffusion model for determining radon diffusion parameters and estimation of exhalation of radon from uranium tailings piles.

Overall, radon fluxes determined by charcoal adsorption yielded values that averaged 31% higher than those obtained by the in-situ method. Higher average fluxes were strongly influenced by measurements at locations KM-5, -6, and -7 where charcoal fluxes were respectively 93, 112, and 59% above those determined by the in-situ method. In addition, comparatively high values were obtained at the UN-HP tailings pile at locations UN-2, -7, and -8. Conversely, the charcoal adsorption method indicated lower fluxes than the in-situ method at UN-1, -5, -9, and -10.

Although not included as an objective of this study, some results have evolved relative to the field use of charcoal canisters that warrant comment. Seven canisters were situated as shown in Fig. 12 at a distance of 1 m from hole UN-1B, and all were exposed for 21.1 hr. The radon fluxes computed from counting rate data, also given in Fig. 12, show a variation of a factor of nearly two in the four collectors that were clustered; however, excellent agreement of radon flux was provided between the remaining three locations. As all of these collectors were emplaced, exposed, and handled in exactly the same manner, differences in the quantities of radon collected, therefore, had to result in different radon exhalation rates at the specific collection sites. The fact that these differences

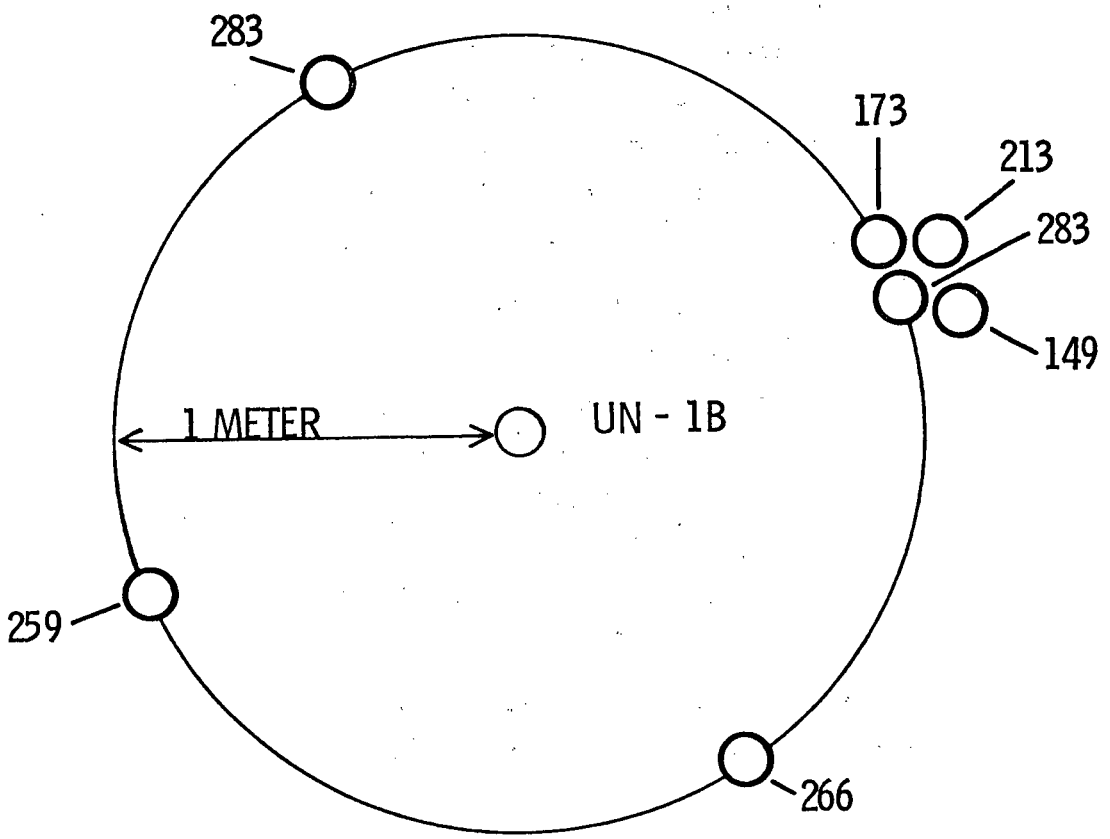

FIGURE 12. Exposure Pattern of Charcoal Canisters and Radon Fluxes at UN-1B

occurred within a very small area, less than 200 cm^2, raises considerable question of the validity of attempting to employ single small area collectors, such as the charcoal canisters, to obtain reasonable estimates of exhalation rates representative of general tailings areas.

At the same time that charcoal samplers were exposed for approximately one day intervals, other canisters were concurrently exposed for periods of several days to two weeks. The exposure conditions and fluxes calculated for these charcoal canisters are given in Table 5. This was done in an attempt to utilize the charcoal adsorber as an integrating medium for long-term radon collection, and therefore provide data that would be more directly comparable to the in-situ method. In addition, we had hoped to use the long exposure charcoal samples as a check on the daily samples, for they should contain the same cumulative quantities of radon as the daily samples altered only by radioactive decay of the collected radon. As graphically depicted in Fig. 13, where the exposure periods of the charcoal canisters at four locations are plotted against the fluxes calculated for those exposure periods, the longer exposures almost universally resulted in reduced values. Countess[5] reported that radon collection efficiency for these canisters was maintained for exposure periods of several days and that adsorption of up to 16 g of water affected the canister capacity for radon by less than 10%. We too verified the continued adsorption efficiency for radon by laboratory exposure of charcoal canisters to dry tailings material for 72 hr. Our field data, however, suggest that long-term exposure of charcoal adsorbers will not provide reasonable estimates of radon flux, and generally underestimates the flux derived by integration of sequential short-term canister exposures by a factor of up to 2.

Also included in Fig. 13 are the values for radon flux obtained by the in-situ method. It is apparent here, and as noted in the prior discussion of the data, that disparities were found in the radon fluxes determined by the two methods. The in-situ method gave higher flux values at UN-13 and considerably lower values at UN-12, KM-5, KM-6, and KM-7 than were obtained with the charcoal canisters. Possible reasons for these differences are many and were not investigated in this work. As the in-situ method was validated by comparison with the actual quantities of radium and radon present in the soil column, we feel these represent true values of the radon exhalation. Thus the different flux values from charcoal canister data suggest

TABLE 5

RADON FLUXES DETERMINED BY CHARCOAL CANISTER ADSORPTION

Location	Date	Time	Exposure (hr)	J atoms / $cm^2 \cdot sec$
UN-1	3/20/78	1757	5.2	70
UN-1B-1	3/5/79	1027	21.1	173
-2	3/5/79	1027	21.1	213
-3	3/5/79	1027	21.1	283
-4	3/5/79	1027	21.1	149
-5	3/5/79	1027	21.1	266
-6	3/5/79	1027	21.1	259
-7	3/5/79	1027	21.1	283
	5/9/79	1200	50	80
	5/9/79	1200	119	140
	5/9/79	1200	119	90
	5/10/79	1410	25.5	130
	5/10/79	1410	145	30
	5/11/79	1450	25	120
	5/11/79	1450	170	60
	5/12/79	0800	17	120
	5/12/79	0800	187	50
	5/13/79	1100	27	120
	5/13/79	1100	214	70
	5/15/79	1530	52	90
	5/15/79	1530	266	60
	5/15/79	1530	266	80
	5/16/79	1800	27	80
	5/16/79	1800	293	80
	5/17/79	1300	312	90
	5/17/79	1300	312	80
	5/18/79	1300	19	100
UN-2	3/20/78	1800	5.7	200
UN-3	3/20/78	1800	5.5	40
UN-5	3/23/78	1900	11.3	50
UN-7	3/23/78	0700	17.7	130
UN-8	3/23/78	1900	11.2	100
UN-9	3/21/78	1800	6.8	120
UN-10	3/23/78	1900	11.3	80

TABLE 5 (continued)
RADON FLUXES DETERMINED BY CHARCOAL CANISTER ADSORPTION (continued)

Location	Date	Time	Exposure (hr)	J atoms $cm^2 \cdot sec$
UN-11	3/23/78	0700	22.4	180
UN-12	10/26/78	2300	5.5	140
	10/27/78	2900	10.6	180
	10/27/78	1900	9.5	250
	10/28/78	0500	12.8	700
	10/28/78	2200	13.5	150
	10/29/78	0800	10.8	480
	10/30/78	0900	24.8	310
	10/30/78	1900	9.3	450
	5/9/79	0900	48	390
	5/10/79	1500	29	340
	5/11/79	1600	25	410
	5/12/79	1000	18	530
	5/12/79	1000	120	690
	5/13/79	1300	27	410
	5/14/79	0900	21	440
	5/15/79	1200	27	400
	5/16/79	1800	30	460
	5/17/79	1300	20	390
	5/17/79	1300	123	370
	5/17/79	1300	243	200
UN-13	10/26/78	2300	5.7	560
	10/27/78	0930	10.6	330
	10/28/79	0800	13.0	490
	10/28/78	2200	13.5	250
	10/29/78	0830	11.0	350
	10/30/78	0900	24.5	290
	10/30/78	1800	9.3	700
	5/9/79	0900	43	470
	5/10/79	1500	29	540
	5/11/79	1600	25	270
	5/12/79	1000	18	470
	5/12/79	1000	120	410
	5/13/79	1300	27	420
	5/14/79	0900	21	410
	5/15/79	1200	27	410
	5/16/79	1730	30	470
	5/17/79	1300	20	240
	5/17/79	1300	123	410
	5/17/79	1300	243	220

TABLE 5 (continued)
RADON FLUXES DETERMINED BY CHARCOAL CANISTER ADSORPTION (continued)

Location	Date	Time	Exposure (hr)	J atoms $cm^2 \cdot sec$
KM-3	10/27/78	1800	5.6	220
	10/28/78	2100	10.9	170
	10/29/78	1500	9.2	130
	5/17/79	0900	310	110
	5/17/79	0900	310	80
KM-4	10/27/78	1800	5.6	640
	10/28/78	2100	10.9	520
	10/29/78	1800	9.2	830
	5/17/79	0900	310	160
	5/17/79	0900	310	160
KM-5	10/28/78	2100	5.6	140
	10/29/78	1700	7.6	480
	5/7/79	0900	70	170
	5/8/79	0900	24	290
	5/9/79	0800	23	270
	5/10/79	1800	35	200
	5/11/79	0930	14.5	470
	5/12/79	1330	28	260
	5/13/79	0900	20	420
	5/14/79	1300	28	350
	5/15/79	0900	20	390
	5/16/79	1300	28	260
	5/17/79	0930	19.5	360
	5/17/79	0930	97	60
	5/17/79	0930	310	180
KM-6	10/28/78	2100	5.6	410
	10/29/78	1700	7.6	390
	5/7/79	0900	70	460
	5/8/79	0900	24	380
	5/9/79	0800	23	730
	5/10/79	1900	35	540
	5/11/79	1030	16	280
	5/12/79	1300	23	210
	5/13/79	0900	20	250
	5/14/79	1400	29	230
	5/15/79	0800	19	150
	5/16/79	1200	27	200
	5/17/79	0930	21.5	250
	5/17/79	0930	97	230
	5/17/79	0930	310	200

TABLE 5 (continued)
RADON FLUXES DETERMINED BY CHARCOAL CANISTER ADSORPTION (continued)

Location	Date	Time	Exposure (hr)	J atoms / $cm^2 \cdot sec$
KM-7	10/28/78	2030	5.6	250
	10/29/78	1700	7.6	140
	5/7/79	0900	70	150
	5/9/79	0800	23	260
	5/10/79	1810	34	210
	5/11/79	1130	17	220
	5/12/79	1200	24	220
	5/13/79	0900	21	210
	5/14/79	1530	31	180
	5/15/79	0900	17	270
	5/16/79	1000	25	210
	5/17/79	0930	24	250
	5/17/79	0930	97	210
	5/17/79	0930	310	120

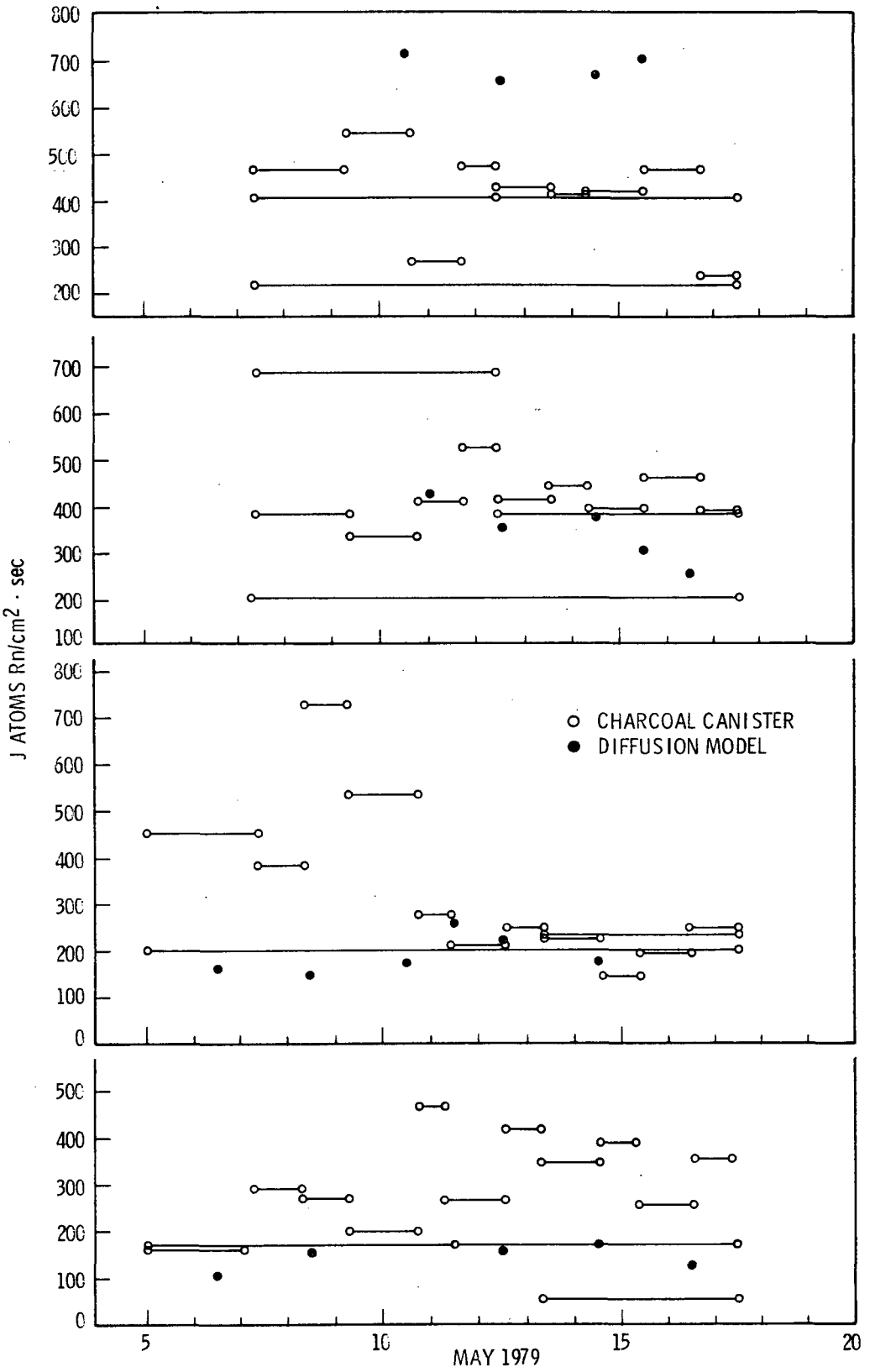

FIGURE 13. Radon-222 Fluxes Measured by Different Methods

that some parameter such as different local source strength, physical enhancement of the radon exhalation by pedestrian traffic, or perhaps some type of pumping action induced by the charcoal influenced the amount of radon collected by the charcoal. At any rate, it appears from these data that the charcoal canister method for determining radon flux can provide useful survey type data with short-term exposures, but should receive careful scrutiny before adoption as a method for determining absolute radon exhalation from tailings materials.

TOTAL RADON EXHALATION FROM A URANIUM TAILINGS PILE

The two uranium tailings piles are sources from which radon is delivered to the atmosphere and transferred by winds offsite from the mill property. In order to make assessment of the radiological consequences of this emission, knowledge of the magnitude of the source term is required. Estimates of the integrated radon release, shown in Table 6, were obtained from the product of the average of all the fluxes measured for a given tailings region and the total area of this region. It is realized that a calculation of this nature is fraught with uncertainties, primarily the assumption that the few measurements made are representative of the entire tailings pile. As an example, the surface radium concentrations at the dry beach locations at UN-HP varied from 7 to 38 dps/cm^3, although the total radium inventory was considerably more uniform. Calculated radon fluxes varied from 70 to 420 atoms/$cm^2 \cdot$sec with the resultant average of 260 atoms/$cm^2 \cdot$sec. With recognition of such limitations, it was estimated that 6.4 and 7.8 Ci/day of radon were exhaled from the carbonate and acid leach tailings areas studied, which converted to respective areal emissions of 14 and 7.1 Ci/day/km^2. We re-emphasize that the 14 Ci/day/km^2 value calculated from UN-HP tailings was based solely on the relatively dry standby side of the tailings pile. If the wet side of the pile, which actively received the tailings slurry, is considered, an areal exhalation of about 8 Ci/day/km^2 was calculated based on estimates of the surface areas covered by solution, wet beach, etc., and the radon exhalation rates for these areas.

TABLE 6

RADON EXHALATION FROM URANIUM TAILINGS PILES

		UN-HP Carbonate Leach			Kerr-McGee Acid Leach	
	J atoms/cm^2/sec	Area cm^2	E (total) atoms/sec	J	Area	E
Wet beach 3,7,8	80	0.5×10^9	4.0×10^{10}	60	1.1×10^9	0.7×10^{11}
Dry beach 1,2,5,10	260	3.4×10^9	8.9×10^{11}	190	4.6×10^9	8.7×10^{11}
Berm 6,9,11	320	0.6×10^9	1.9×10^{11}	180	2.4×10^9	4.3×10^{11}
			Σ 1.13×10^{12} atoms/sec			Σ 1.37×10^{12}
		or	$\sim$6.4 Ci/day			$\sim$7.8 Ci/day
		or	$\sim$14 Ci/day/km^2*			$\sim$7.1 Ci/day/km^2

*NOTE: This value is only for the relatively dry standby side of the UN-HP pile. Exhalation per unit area for the full pile would be significantly lower due to much more extensive solution area and the increased proportion of wet beach in the active side of the tailings pile.

RADON FROM AN ABANDONED TAILINGS PILE

An unused tailings pile resulting from alkaline leach milling operations predating the current mill at the United Nuclear-Homestake Partners' property at Grants, New Mexico, provided an opportunity to study radon movement in circumstances similar to those present at numerous inactive mill

tailings sites. These tailings comprise the pentagonal area shown in Fig. 1, and test holes were implanted as shown in Fig. 3. The UN-12 hole was in an area that was devoid of vegetation; and UN-13 was located 40 m from the first hole in an area that had been sparsely revegetated with Four-wing Saltbush (*Atriplex canescens*). Considering the proximity of these two locations, and the manner of addition of the tailings slurry to the pile, it was presumed that these two areas had received the same tailings, although the horizon could easily have been altered over the years by wind erosion. Soil moisture content at these two locations was determined gravimetrically on grab samples of material removed when the holes were drilled. A fairly uniform moisture content of 11% was found throughout UN-12 and below 100 cm depth in UN-13. The top of the soil column at UN-13 had a moisture content of about 5%.

Results obtained from gamma logging of these two test holes are given in Appendix 1. From the plots of the pooled radium data shown in Figs. 14 and 15, it can be seen that below 20 cm radium concentrations at UN-12 are somewhat higher than at UN-13 and significantly higher in the top 20 cm.

These data were evaluated by the diffusion model [Equations (19) and (16)] to determine the diffusion coefficients, emanation factors, and the fluxes of radon escaping the tailings given in Table 7.

TABLE 7

RADON DIFFUSION AND FLUX AT AN INACTIVE TAILINGS PILE

Sampling Location	Date	α Fraction	D cm^2/sec	J $atoms/cm^2/sec$
UN-12	10/26/78	0.33±.03	0.0050±.0016	410±60
	10/30/78	0.24±.03	0.0018±.0010	190±50
	5/10/79	0.37±.03	0.0043±.0014	420±60
	5/12/79	0.34±.03	0.0035±.0013	350±60
	5/14/79	0.34±.03	0.0040±.0021	380±90
	5/15/79	0.36±.02	0.0023±.0008	300±50
	5/16/79	0.33±.03	0.0019±.0007	250±50
UN-13	10/26/78	0.34±.03	0.0177±.0076	770±120
	10/30/78	0.31±.03	0.0170±.0081	680±110
	5/10/79	0.41±.03	0.0105±.0035	710±100
	5/12/79	0.44±.03	0.0077±.0024	660±90
	5/14/79	0.39±.03	0.0097±.0034	670±100
	5/15/79	0.39±.03	0.0109±.0039	700±110

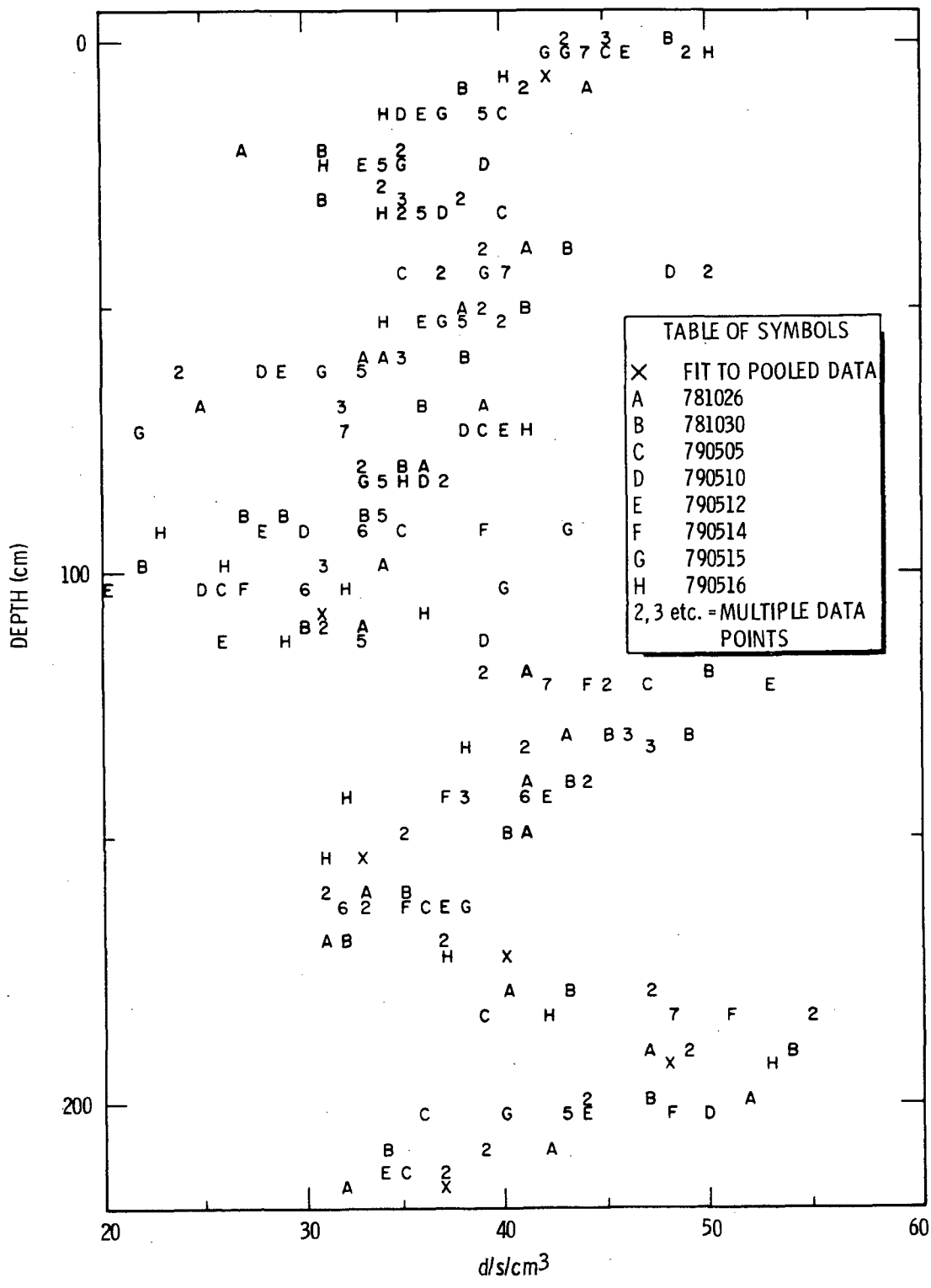

FIGURE 14. Radium Concentrations, UN-12

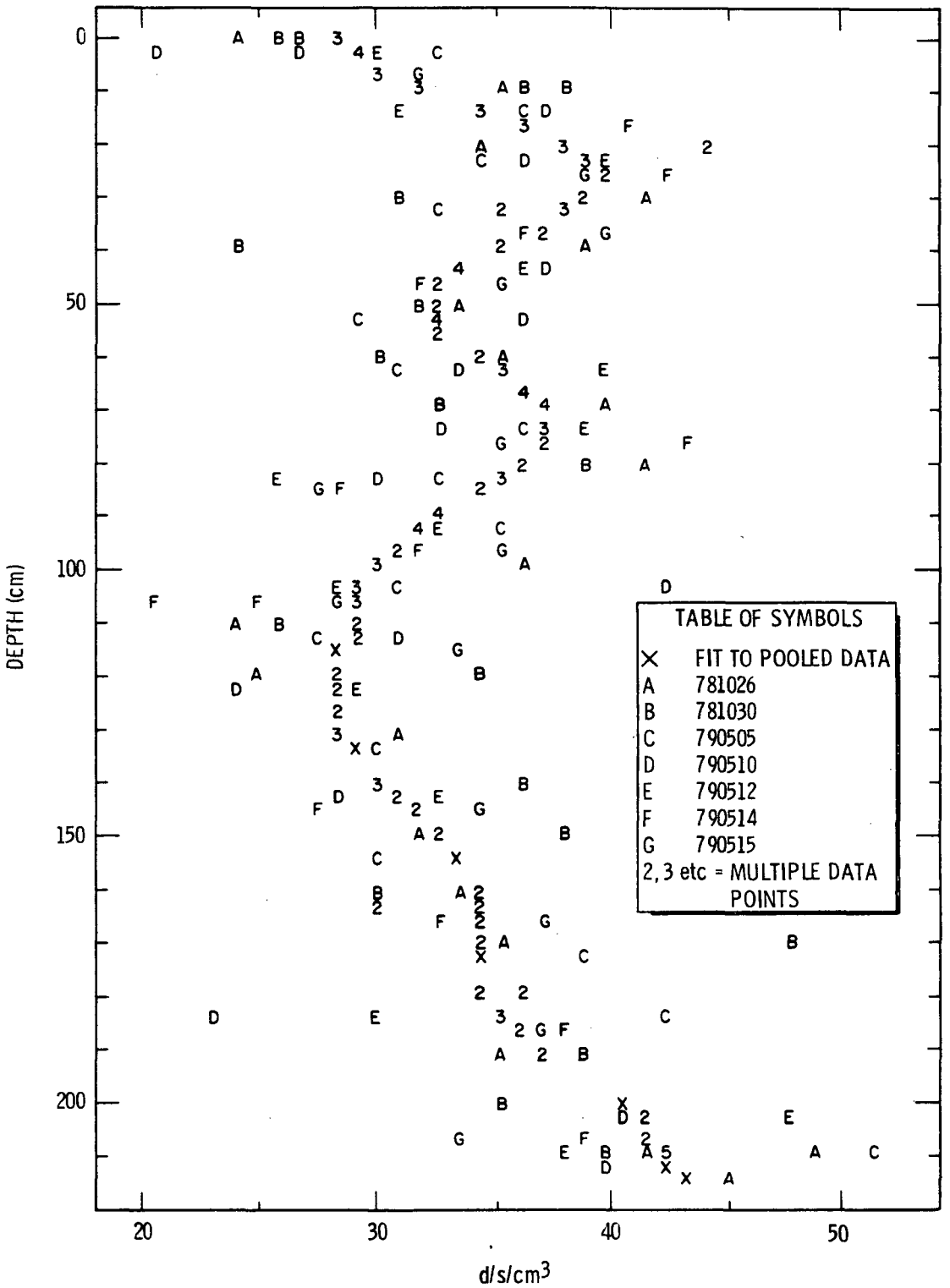

FIGURE 15. Radium Concentrations, UN-13

It is interesting to note that the diffusion coefficient at UN-12 is about the same as a dry beach area in the active UN-HP tailings pile. Higher rates of diffusion were noted at UN-13, comparable to those found in the berm locations in an active pile, even though by external appearance the tailings were not significantly different from those at UN-12. Resultant radon exhalation at UN-13 was nearly double that found at UN-12, in spite of the lower rate of radon production. It is possible that the increased rate of radon transport was due entirely to the existing differences in moisture content of the surface tailings. This seems very unlikely based on comparisons of diffusion and exhalation differences arising from tailings columns with similar moisture contents in the active tailings piles. The fact that this hole was located in a vegetated area suggests the intriguing possibility that the increased radon movement resulted from disturbance of the tailings column by the root systems, by providing air channels adjacent to capillary roots or gross air passages resulting from decayed roots. The decreased surface soil moisture content at UN-13 can probably be ascribed to water uptake by the plants. It is beyond the scope of this study to define the mechanisms involved; however, let it suffice that significantly more radon was found to escape a tailings surface that was vegetated than one that had no vegetation. As one method for stabilizing tailings against erosive forces is to establish a vegetative cover, such application might significantly increase the quantities of radon exhaled by a stabilized pile, thus compromising one of the prime objectives of the stabilization effort.

EFFECTS OF ATMOSPHERIC VARIABLES ON RADON EXHALATION

One of the objectives of this study was to evaluate the influence of meteorological parameters on exhalation of radon from the uranium tailings piles. Clements and Wilkening[12] found that atmospheric pressure changes of a few percent occurring over 1-2 day periods resulted in changes of as great as 60% in the radon flux from alluvial soil. Kraner, et al[3] also reported an inverse correlation between radon flux and barometric pressure changes, and described the observed changes as a piston effect involving pressure-induced vertical displacement of the soil gas. Kraner, et al[3] also found

evidence of depletion of radon concentrations in soil gas to depths of 1 m, and reported a somewhat higher radon flux during periods of high wind.

Conditions during May 1979 were ideal for field evaluation of the combined influence of changes of barometric pressure and wind speed on the flux of radon across the soil-air interface. As seen in Fig. 16, commencing on May 5 a falling barometer was accompanied by a period of very high winds. The barometer started to rise on May 10 and wind speeds moderated significantly. The radon concentration profiles determined at UN-9B during this time are shown in Fig. 17, and certainly provide no direct evidence that radon concentrations were altered by meteorological changes. Within counting statistics, these profiles were identical. During the period of high winds subsequent to logging on May 5, 37 cm of tailings were eroded from the surface at this location, which is shown as the terminus of the subsequent data. The sampling on May 15 was also conducted during a period of high winds; in fact, a peak gust of 36 m/sec was recorded during sampling. No changes in the radon concentrations were observed even in the surface layers of the tailings material. A radon emanation coefficient of 0.36 was determined for the tailings at this location, so at least any gross changes occurring in free radon distributions resulting from any external influence should have been apparent. There were no such effects observed.

The radon flux data derived from both calculation and from charcoal canister data accumulated from all sampling locations at the active and inactive piles were analyzed statistically to evaluate flux response to changes in barometric pressure and wind velocity. To do this, we regressed radon flux data on the pressure and wind speed and found that these two variables did not significantly affect radon flux determined by any of the three methods. Again, it is emphasized that fluxes calculated by both the diffusion model and mass balance represent average values resulting from radon diffusion integrated over an extended period, and as such, quite possibly do not provide sufficient sensitivity to accommodate short-term fluctuations. In any case, it appears that any short-term variations do not greatly influence the overall exhalation of radon from the uranium tailings piles studied.

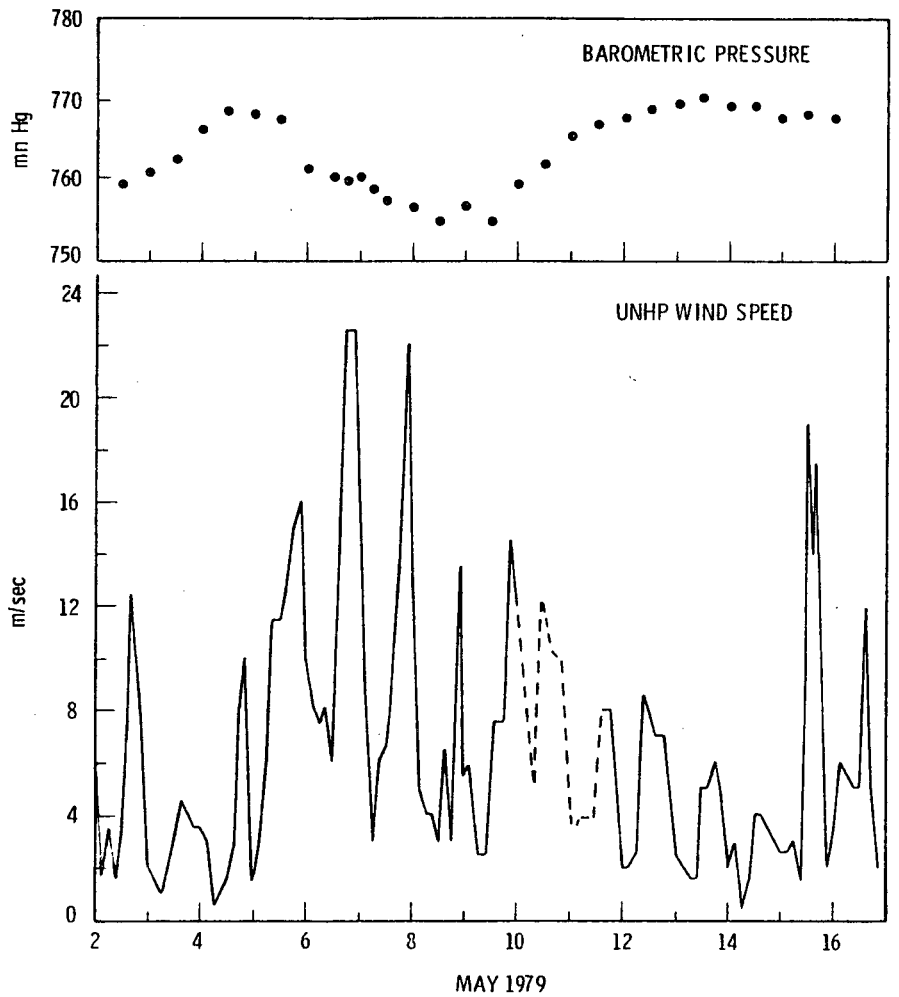

FIGURE 16. Wind Speed and Barometric Pressure - May 1979

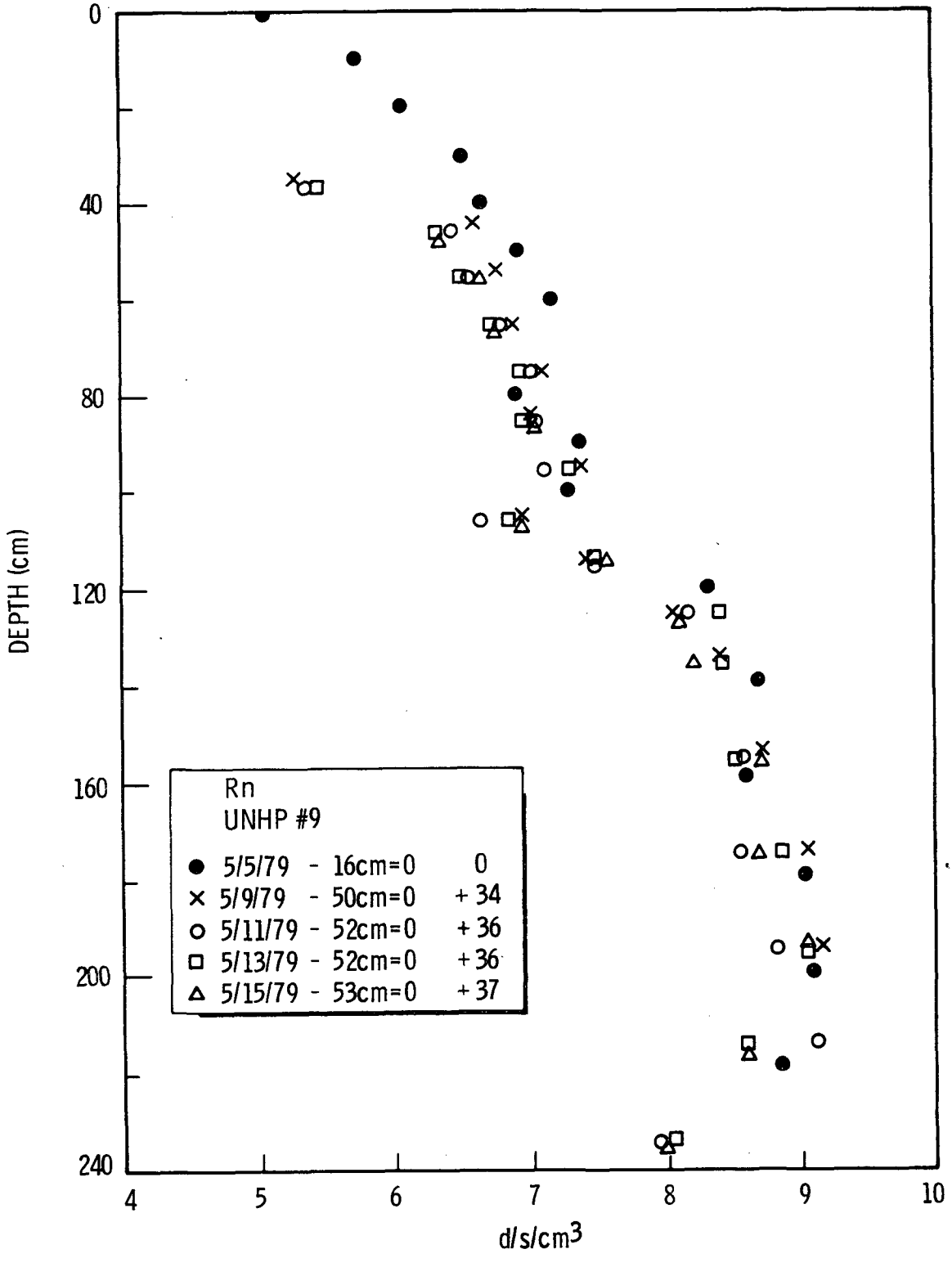

FIGURE 17. Measured Radon-222 Concentrations, UN-9

REFERENCES

1. Tanner, A. B., "Radon Migration in the Ground: A Review." In The Natural Radiation Environment, J.A.S. Adams and W. M. Landers, Eds., University of Chicago Press, Chicago, IL (1964).

2. Tanner, A. B., "Radon Migration in the Ground: A Supplementary Review." Proceedings of The Natural Radiation Environment III Symposium. To be published.

3. Kraner, H. W., G. L. Schroeder, and R. D. Evans, "Measurements of the Effects of Atmospheric Variables on Radon-222 Flux and Soil Gas Concentrations." In The Natural Radiation Environment, pp. 191-215, University of Chicago Press, Chicago, IL (1964).

4. Wilkening, M. H., W. E. Clements, and D. Stanley. "Radon-222 Flux Measurements in Widely Separated Regions." In The Natural Radiation Environment II, pp. 717-730, CONF-720805-P2, NTIS, U. S. Department of Commerce (1975).

5. Countess, R. J., "^{222}Rn Flux Measurement with a Charcoal Canister." Health Phys., 31:455 (1976).

6. Megumi, Kazuko, and T. Mumuro, "A Method for Measuring Radon and Thorium Exhalation from the Ground." J. Geo. Phys. Res. 77:3052 (1972).

7. Kirichenko, L. V., "Radon Exhalation from Vast Areas According to Vertical Distribution of Its Short-Lived Decay Products." J. Geo. Phys. Res. 75:3639 (1970).

8. Pearson, J. E. and G. E. Jones, "Soil Concentrations of Emanating Radium-226 and the Emanation of Radon from Soils and Plants." Tellus 18:1 (1966).

9. Macbeth, P. J., C. M. Jensen, V. C. Rogers, and R. F. Overmeyer. Laboratory Research on Tailings Stabilization Methods and Their Effectiveness in Radiation Containment, Department of Energy Report GJT-21 (1978).

10. Wogman, N. A., D. E. Robertson, and R. W. Perkins, "A Large Detector, Anticoincidence Shielded Multidimensional Gamma-Ray Spectrometer." Nucl. Instrum. Meth. 50:1 (1967).

11. Culot, M.V.J., H. G. Olson, and K. J. Schiager, "Effective Diffusion Coefficient of Radon in Concrete: Theory and Method of Field Measurements." Health Phys. 30:263-270 (1976).

12. Clements, W. E. and M. H. Wilkening, "Atmospheric Pressure Effects on ^{222}Rn Transport Across the Earth-Air Interface." J. Geo. Phys. Res. 79:5025-5029 (1974).

13. Silker, W. B., N. A. Wogman, C. W. Thomas, D. B. Carr, and P. C. Heasler, "Measurement of Radon Diffusion and Exhalation from Uranium Tailings Piles." Env. Sci. and Tech. 13:962-964 (1979).

APPENDIX

Sample Location UN-1 12-6-77

Depth Correction .0

	Radium		Radon	
Depth	DPS/CM^3	Var.	DPS/CM^3	Var.
0	9.5	.6	4.50	.00
4	9.7	.5	4.55	.00
10	8.9	.4	4.51	.00
15	9.4	.4	4.62	.00
25	9.8	.5	5.62	.00
35	10.6	.6	7.54	.00
40	13.0	.7	8.64	.00
45	12.6	.8	9.98	.00
50	15.4	.9	11.00	.00
55	13.7	.9	11.80	.00
60	14.0	1.0	12.46	.01
65	14.2	1.0	13.15	.01
70	16.9	1.1	13.82	.01
75	14.4	1.1	14.88	.01
85	17.8	1.1	15.60	.01
95	11.7	.9	13.16	.01
99	11.5	.9	11.80	.00

Sample Location UN-1 3-20-78

Depth Correction 3.0

	Radium		Radon	
Depth	DPS/CM^3	Var.	DPS/CM^3	Var.
3	10.0	1.2	4.24	.01
8	7.8	1.2	4.50	.01
13	9.0	1.4	5.21	.01
18	6.7	1.5	5.58	.01
23	7.5	1.8	6.25	.01
33	11.7	2.3	8.77	.02
43	15.3	2.8	11.68	.02
48	15.6	2.9	12.12	.03
58	12.0	3.2	13.33	.03
68	17.2	3.5	15.53	.03
78	15.0	3.6	16.28	.03
88	17.5	2.9	13.69	.03
98	10.6	2.2	9.16	.02

Sample Location UN-1B 5-5-79

Depth Correction .0

	Radium		Radon	
Depth	DPS/CM^3	Var.	DPS/CM^3	Var.
0	7.5	.8	4.93	.00
10	8.3	1.0	5.06	.00
20	17.4	1.5	10.43	.01
30	17.3	1.6	11.27	.01
40	13.5	1.7	11.31	.01
40	15.0	1.7	11.24	.01
50	16.4	1.8	12.37	.01
60	11.4	1.8	10.57	.01
70	11.8	2.0	12.23	.02
80	19.9	2.5	17.70	.02
90	17.2	2.8	16.77	.02
100	23.7	3.1	20.84	.03
120	18.5	3.4	20.51	.03
140	26.5	3.2	22.94	.03
160	13.4	1.9	12.64	.02
180	16.3	1.9	14.39	.02
200	10.2	1.8	11.57	.01
220	7.9	1.6	8.86	.01
240	6.9	1.7	7.30	.01
260	12.4	1.9	11.36	.01
280	15.4	2.2	12.85	.02
293	16.3	2.4	16.18	.02

Sample Location UN-1B 5-9-79

Depth Correction 2.0

	Radium		Radon	
Depth	DPS/CM^3	Var.	DPS/CM^3	Var.
2	6.9	2.1	3.80	.02
2	6.0	.7	3.52	.00
12	11.8	1.0	6.82	.01
22	17.0	5.1	10.47	.05
32	13.2	5.1	10.62	.05
42	13.8	5.1	10.79	.05
42	17.8	5.4	11.86	.05
52	15.6	5.4	11.67	.05
62	11.1	5.5	9.65	.05
72	13.7	6.2	11.91	.06
82	18.1	7.9	17.73	.08
92	18.2	8.5	16.60	.08
102	27.0	9.5	20.56	.10
122	24.0	10.2	21.36	.10
142	26.3	9.7	23.06	.10
162	14.4	5.9	12.92	.06
182	15.7	5.9	14.37	.06
202	13.3	5.4	11.38	.05
222	6.4	4.9	9.23	.04

Sample Location UN-1B 5-11-79

Depth Correction 6.0

	Radium		Radon	
Depth	DPS/CM^3	Var.	DPS/CM^3	Var.
6	6.2	1.3	4.47	.01
16	11.8	1.8	7.54	.01
26	14.9	5.0	11.12	.05
36	11.7	5.0	10.77	.05
46	15.7	5.2	10.77	.05
56	12.0	5.4	10.57	.05
66	9.9	5.7	10.99	.05
76	15.4	7.1	14.42	.07
86	20.5	8.2	16.37	.08
96	21.1	8.9	18.23	.09
106	20.5	9.9	23.06	.11
126	30.6	11.2	25.76	.12
146	13.0	7.6	14.90	.07
166	16.9	5.6	11.99	.05
186	17.8	5.5	11.02	.05
206	12.0	5.4	10.88	.05

Sample Location UN-1B 5-13-79

Depth Correction 6.0

	Radium		Radon	
Depth	DPS/CM^3	Var.	DPS/CM^3	Var.
6	6.1	.8	4.18	.00
16	11.6	1.2	7.61	.01
26	22.4	5.2	12.41	.05
36	13.7	5.0	10.22	.05
46	13.3	5.3	11.64	.05
56	9.2	5.5	11.43	.05
66	9.2	6.0	11.31	.06
76	11.2	7.0	14.90	.07
86	24.9	8.2	16.81	.08
96	16.3	8.9	17.89	.09
106	22.4	10.0	23.26	.11
126	22.9	11.0	24.89	.12
146	16.6	7.6	15.21	.07
166	13.8	5.7	12.55	.05
186	14.0	5.6	11.49	.05
206	13.1	5.4	10.91	.05

Sample Location KM-1 3-25-78

Depth Correction .0

	Radium		Radon	
Depth	DPS/CM^3	Var.	DPS/CM^3	Var.
0	17.1	3.4	14.74	.03
5	19.1	3.2	13.71	.03
10	14.5	3.2	12.87	.03
15	15.0	6.7	13.38	.06
20	12.4	7.1	15.27	.07
25	22.4	7.1	16.77	.07
30	14.9	6.8	15.45	.07
35	11.8	6.3	12.15	.06
40	11.1	6.0	12.29	.06
50	4.8	5.6	12.03	.05
55	13.4	5.6	11.72	.05
65	8.0	5.8	12.83	.06
75	7.5	5.9	11.67	.06
83	14.7	6.1	13.31	.06

Sample Location UN-2 12-7-77

Depth Correction .0

	Radium		Radon	
Depth	DPS/CM^3	Var.	DPS/CM^3	Var.
210	10.8	3.1	12.70	.03
199	12.0	3.4	15.36	.03
179	14.3	3.1	12.70	.03
159	11.3	2.6	10.69	.02
139	8.3	2.7	9.92	.02
139	9.2	2.7	10.21	.02
139	11.6	2.7	10.03	.02
129	12.0	3.0	11.46	.03
119	10.9	3.1	11.03	.03
109	9.2	3.0	10.04	.02
99	13.0	2.8	9.55	.02
89	10.6	2.8	10.77	.02
79	12.0	2.8	11.26	.02
69	16.7	3.0	12.26	.03
59	14.1	3.3	13.37	.03
49	13.3	3.3	13.20	.03
39	12.6	3.0	11.41	.03
29	11.5	2.6	10.61	.02
19	14.7	2.3	10.11	.02
9	11.6	2.5	9.65	.02
4	18.4	3.2	9.78	.02
0	19.4	3.9	9.41	.03

Sample Location UN-2 3-20-78

Depth Correction .0

	Radium		Radon	
Depth	DPS/CM^3	Var.	DPS/CM^3	Var.
0	15.2	2.1	9.53	.02
5	11.4	2.1	8.72	.02
10	14.8	2.2	9.34	.02
15	11.6	2.3	9.17	.02
20	16.3	2.4	9.35	.02
25	14.6	2.6	9.96	.02
30	13.5	2.8	10.58	.02
35	10.9	3.1	12.04	.03
45	12.8	3.5	14.87	.03
55	15.3	3.3	13.71	.03
65	10.8	2.8	11.20	.02
75	10.0	2.7	10.70	.02
85	13.2	2.8	10.90	.02
95	8.4	2.9	9.56	.02
105	9.7	3.3	11.55	.03
115	13.0	3.4	12.82	.03
125	11.4	3.0	12.09	.03
135	7.5	2.5	9.28	.02
155	12.4	2.7	10.57	.02
175	13.9	3.1	12.32	.03
195	13.9	3.4	15.24	.03
211	11.7	2.9	11.01	.02

Sample Location KM-2 3-25-78

Depth Correction .0

	Radium		Radon	
Depth	DPS/CM^3	Var.	DPS/CM^3	Var.
0	16.9	5.9	12.66	.06
5	14.5	6.2	13.44	.06
10	16.2	6.6	13.64	.06
15	11.4	7.1	14.15	.07
20	20.3	7.4	15.28	.07
25	16.0	7.6	15.29	.07
30	26.3	7.9	16.07	.08
35	19.2	8.2	17.57	.08
40	21.4	8.2	16.40	.08
50	17.5	8.7	15.93	.08
60	24.9	10.0	22.44	.10
70	18.5	10.5	18.19	.10
80	25.4	12.4	23.28	.12
90	37.2	15.2	35.66	.16
95	39.5	15.5	37.75	.17
100	36.0	14.6	36.18	.16
105	34.6	12.1	30.14	.13
110	11.0	8.9	14.14	.07
114	7.4	7.4	10.45	.06

Sample Location UN-3 12-7-77

Depth Correction .0

	Radium		Radon	
Depth	DPS/CM^3	Var.	DPS/CM^3	Var.
4	26.4	6.8	20.56	.06
9	26.8	1.8	21.26	.01
14	25.9	1.7	22.21	.01
19	23.7	1.6	21.11	.01
49	---	---	21.48	.02
79	---	---	21.26	.05
109	15.9	3.7	14.05	.03
139	15.8	1.5	16.72	.01
169	---	---	24.22	.02
222	---	---	20.96	.02

Sample Location UN-3 3-20-78

Depth Correction 5.0

	Radium		Radon	
Depth	DPS/CM^3	Var.	DPS/CM^3	Var.
5	30.3	5.1	24.20	.05
10	25.4	5.3	26.06	.06
15	29.4	10.7	25.23	.11
20	28.4	9.8	19.75	.09
25	16.1	9.1	15.30	.08
30	18.8	9.5	17.14	.09
35	16.3	10.9	22.26	.11
40	23.5	11.4	25.02	.12
50	22.5	11.4	26.55	.12
60	21.0	9.4	17.64	.09
70	19.9	10.2	20.63	.10
80	26.7	11.4	29.89	.13
90	15.6	8.1	16.32	.08
100	17.1	6.7	13.33	.06
110	15.0	7.3	13.42	.07
120	16.0	8.9	19.53	.09
130	25.0	9.5	21.10	.10
140	18.2	9.3	19.00	.09
150	22.9	11.1	23.68	.11
160	27.5	13.1	28.80	.14
170	34.8	14.3	33.80	.15
180	28.5	13.9	32.06	.15
190	24.9	12.4	25.99	.13
200	22.3	11.8	24.24	.12
210	23.6	12.0	23.16	.12
220	23.3	13.2	25.17	.13
221	25.1	13.2	24.97	.13

Sample Location UN-4 12-7-77

Depth Correction .0

	Radium		Radon	
Depth	DPS/CM^3	Var.	DPS/CM^3	Var.
1	12.7	2.4	9.40	.02
6	15.4	2.1	11.52	.01
11	19.1	4.0	14.11	.03
16	14.4	4.4	16.08	.04
21	22.3	4.7	17.95	.04
26	22.1	5.3	19.63	.05
31	---	---	20.05	.06
36	---	---	19.50	.06
41	---	---	21.64	.07
46	---	---	21.94	.07

Sample Location UN-4 3-21-78

Depth Correction .0

	Radium		Radon	
Depth	DPS/CM^3	Var.	DPS/CM^3	Var.
0	12.2	7.1	11.80	.07
5	17.3	8.3	15.98	.08
10	21.7	10.0	20.10	.10
15	19.0	11.1	23.17	.11
20	23.2	11.9	24.81	.12
25	26.1	12.9	25.16	.13
30	32.3	13.7	27.06	.14
35	28.5	14.5	29.50	.15
40	30.7	15.4	32.01	.16
45	39.4	15.8	32.18	.16
50	30.7	16.1	33.33	.16
60	34.9	16.3	33.18	.16
70	38.6	16.2	34.55	.16
80	29.7	15.1	30.22	.15
90	37.5	14.8	28.28	.14
100	30.8	14.9	29.74	.15
110	38.9	14.9	31.31	.15
120	31.2	14.5	27.98	.14
130	37.8	15.5	30.77	.15
140	35.0	17.3	36.98	.18
150	33.3	18.0	37.16	.18
160	36.0	18.8	39.01	.19
170	39.6	19.6	40.64	.20
180	42.5	19.7	42.02	.21
190	38.5	19.1	40.75	.20
200	38.3	17.8	36.52	.18
210	41.2	16.8	34.36	.17
230	32.0	16.0	33.26	.16

Sample Location KM-4 10-28-78

Depth Correction .0

	Radium		Radon	
Depth	DPS/CM^3	Var.	DPS/CM^3	Var.
0	18.7	2.7	13.16	.03
10	15.2	3.1	13.74	.03
20	14.8	3.3	14.59	.03
30	20.3	3.3	14.58	.03
40	18.9	3.3	13.94	.03
50	18.3	3.3	13.58	.03
60	16.4	3.5	14.43	.03
70	16.7	3.5	15.07	.03
80	16.9	3.5	14.74	.03
90	13.0	3.4	13.90	.03
100	15.8	3.3	12.49	.03
0	15.1	2.7	13.67	.03
100	14.5	3.3	12.67	.03
110	12.7	3.3	12.66	.03
110	11.3	3.3	12.68	.03
120	15.6	3.5	14.05	.03
130	16.8	3.5	14.02	.03
140	15.8	3.6	14.58	.03
150	17.4	3.7	15.19	.04
160	14.7	3.7	15.53	.03
170	15.5	3.6	14.96	.03
180	16.1	3.5	14.33	.03
190	12.9	3.5	14.39	.03
200	14.8	3.5	14.24	.03
210	16.0	3.4	15.38	.03
220	18.1	3.6	15.41	.03
228	11.3	3.4	14.57	.03
10	15.5	3.1	14.30	.03
10	17.7	6.3	14.03	.06
10	16.5	6.2	13.98	.06
10	16.8	6.3	14.15	.06
10	16.9	6.2	14.05	.06
10	20.4	6.2	14.06	.06
10	19.6	6.3	14.17	.06
10	17.1	6.3	13.93	.06
10	21.5	6.3	14.30	.06
10	15.1	6.3	14.27	.06
10	16.5	6.3	14.03	.06

Sample Location UN-5 12-8-77

Depth Correction .0

	Radium		Radon	
Depth	DPS/CM^3	Var.	DPS/CM^3	Var.
4	35.0	10.1	21.11	.10
9	33.6	7.6	19.76	.08
14	29.5	6.7	18.50	.07
19	20.6	6.3	17.38	.06
29	23.1	5.7	15.59	.06
39	15.5	5.5	14.58	.05
49	16.3	5.3	14.61	.05
59	13.7	5.1	13.43	.05
69	17.6	5.0	13.37	.05
79	19.5	5.2	13.07	.05
89	18.8	5.5	12.97	.05
99	20.6	5.9	13.90	.06
109	10.2	6.2	14.56	.06
119	11.9	6.1	13.55	.06
129	14.0	6.1	14.18	.06
139	19.8	6.6	15.22	.06
149	16.0	6.6	15.95	.06
159	13.6	6.5	16.30	.06
169	20.5	6.4	15.17	.06
179	17.0	6.4	15.41	.06
189	19.4	6.8	16.33	.07
199	14.9	6.9	16.07	.07
209	18.3	7.1	16.32	.07
219	16.4	7.7	17.63	.08

Sample Location UN-5 3-23-78

Depth Correction 2.0

	Radium		Radon	
Depth	DPS/CM^3	Var.	DPS/CM^3	Var.
2	34.1	7.7	18.22	.08
7	42.3	7.6	17.24	.07
12	28.9	7.1	17.14	.07
17	17.0	6.5	13.51	.06
22	11.1	6.0	11.21	.05
27	11.3	5.8	11.50	.05
32	10.9	5.9	11.83	.05
37	18.6	6.0	13.38	.06
42	15.1	5.9	14.26	.06
52	14.6	5.4	10.73	.05
62	12.0	5.6	11.05	.05
72	14.2	6.1	12.94	.06
82	17.1	6.7	13.15	.06
92	12.3	7.2	14.73	.07
102	17.5	7.8	16.53	.08
112	12.6	7.4	13.53	.07
122	17.3	7.3	13.62	.07
142	19.3	8.3	17.06	.08
162	16.9	7.6	16.47	.07
182	17.8	8.1	16.90	.08
202	17.2	8.4	16.90	.08
219	19.1	10.1	21.51	.10

Sample Location KM-5 10-28-78

Depth Correction .0

	Radium		Radon	
Depth	DPS/CM^3	Var.	DPS/CM^3	Var.
0	20.9	10.4	23.70	.11
10	34.1	12.3	27.57	.13
20	39.3	12.7	31.14	.14
30	17.2	9.4	17.42	.09
40	17.8	4.2	18.00	.04
50	10.0	4.0	14.52	.03
60	12.5	4.3	16.42	.04
70	23.5	5.0	21.50	.05
80	21.6	4.8	21.44	.05
90	17.5	3.9	16.68	.03
100	12.5	2.8	9.37	.02
110	7.3	2.5	10.03	.02
110	10.9	2.5	10.10	.02
120	11.3	2.4	10.23	.02
120	10.3	2.4	9.67	.02
130	9.1	2.2	8.87	.02
140	6.9	2.3	8.82	.02
150	9.8	2.7	11.67	.02
160	13.4	3.3	14.97	.03
170	12.6	3.2	14.58	.03
180	11.2	3.1	13.53	.03
190	12.8	3.0	13.16	.03
198	10.4	2.9	12.55	.03
110	10.6	2.5	10.46	.02
50	15.1	4.0	14.58	.03
60	17.2	4.2	15.81	.04
70	23.3	5.0	21.91	.05

Sample Location KM-5 5-6-79

Depth Correction 3.0

	Radium		Radon	
Depth	DPS/CM^3	Var.	DPS/CM^3	Var.
3	28.4	12.0	27.21	.13
3	39.0	12.0	27.49	.17
13	42.9	13.9	34.32	.15
23	28.9	12.3	26.17	.13
33	19.7	9.8	18.40	.09
43	15.4	9.3	18.83	.09
53	18.0	9.0	16.82	.09
63	20.1	10.2	19.57	.10
73	26.8	11.2	25.07	.12
83	18.3	10.0	21.32	.10
93	11.1	7.4	14.00	.07
103	9.0	5.6	10.01	.05
123	8.0	4.7	10.12	.04
143	8.8	5.0	9.75	.05
163	13.7	6.7	15.29	.07
183	11.3	6.3	14.67	.06
193	14.4	5.8	11.93	.05

Sample Location KM-5 5-8-79

Depth Correction 3.0

	Radium		Radon	
Depth	DPS/CM^3	Var.	DPS/CM^3	Var.
3	36.2	12.0	26.93	.13
13	42.5	14.4	34.08	.15
23	28.2	12.1	25.05	.12
33	15.3	9.6	18.43	.09
43	21.4	9.2	18.20	.09
53	18.7	9.0	15.96	.08
63	16.4	10.0	19.43	.10
73	27.5	11.2	25.04	.12
83	17.8	10.1	17.73	.10
93	13.0	7.5	14.38	.07
103	11.4	5.5	9.93	.05
123	10.7	4.7	10.33	.04
143	7.7	4.8	9.97	.05
163	14.8	6.2	14.85	.07
183	7.0	6.2	14.37	.06
183	9.6	6.2	14.07	.06
193	11.5	5.6	11.61	.05

Sample Location KM-5 5-11-79

Depth Correction 3.0

	Radium		Radon	
Depth	DPS/CM^3	Var.	DPS/CM^3	Var.
3	38.0	11.8	26.02	.13
13	37.1	13.4	31.51	.15
23	28.8	12.1	26.12	.12
33	25.2	9.9	18.20	.09
43	19.9	9.2	17.54	.09
53	17.9	9.0	15.80	.08
63	18.9	9.9	19.43	.10
73	26.1	11.2	25.21	.12
83	20.2	9.9	20.51	.09
93	15.0	7.1	12.75	.06
103	8.3	5.6	9.66	.05
123	10.5	4.6	9.84	.04
143	13.2	5.9	12.35	.06
163	13.0	6.2	13.24	.06
183	11.3	6.0	11.17	.05
195	13.6	5.6	11.14	.05

Sample Location KM-5 5-12-79

Depth Correction 3.0

	Radium		Radon	
Depth	DPS/CM^3	Var.	DPS/CM^3	Var.
3	29.2	12.5	25.66	.13
13	39.2	13.8	33.09	.15
33	19.7	9.9	17.59	.09
43	18.2	9.3	17.46	.09
53	13.9	8.9	15.77	.08
63	24.5	10.2	19.50	.10
73	27.1	11.2	24.68	.12
83	22.8	9.7	20.65	.10
93	14.5	7.3	13.33	.07
103	13.1	5.5	10.14	.05
123	10.2	4.6	9.77	.04
143	8.9	2.3	8.83	.02
163	12.6	3.2	14.02	.03
183	12.9	3.0	13.29	.03
193	12.9	2.8	11.75	.02
23	26.7	12.1	26.35	.12

Sample Location KM-5 5-14-79

Depth Correction 3.0

	Radium		Radon	
Depth	DPS/CM^3	Var.	DPS/CM^3	Var.
3	34.4	12.1	25.28	.13
13	38.2	13.7	33.85	.15
23	28.4	12.0	25.16	.12
33	15.0	9.7	17.53	.09
43	15.5	9.1	16.55	.09
53	14.2	8.9	15.89	.08
63	19.1	9.8	18.79	.10
73	23.0	11.1	25.14	.12
83	21.6	9.8	20.29	.09
93	10.4	7.3	13.06	.07
103	11.2	5.4	9.87	.05
123	11.8	4.6	9.46	.04
143	7.1	4.7	9.26	.04
163	15.9	6.4	14.60	.06
183	10.5	6.1	14.00	.06
194	8.4	5.7	11.83	.05
93	13.5	7.2	12.58	.06
73	23.5	11.2	24.54	.12
72	26.5	11.1	24.57	.12
69	26.2	11.2	26.08	.11

Sample Location KM-5 5-16-79

Depth Correction 5.0

	Radium		Radon	
Depth	DPS/CM^3	Var.	DPS/CM^3	Var.
5	36.3	12.4	25.79	.13
10	39.6	13.1	29.59	.14
15	39.7	13.9	33.66	.16
20	38.2	13.2	31.54	.14
25	---	---	23.37	.11
30	19.9	10.2	18.94	.09
35	20.4	9.6	18.05	.09
45	15.9	9.0	17.00	.09
55	10.7	9.0	16.36	.08
65	23.1	10.4	20.92	.10
70	24.0	10.9	23.61	.11
75	27.7	11.2	25.63	.12
80	25.8	10.6	22.83	.11
85	17.6	9.4	20.11	.09
95	---	---	11.36	.06
105	---	---	10.47	.05
115	8.3	4.8	9.68	.04
125	10.6	4.6	9.73	.04
135	9.6	4.4	8.14	.04
145	12.2	4.9	10.10	.05
155	---	---	14.58	.06
165	14.4	6.5	14.75	.07
175	14.4	6.3	13.61	.06
185	13.0	6.0	13.56	.06
193	9.2	5.6	11.91	.05
155	12.6	6.2	14.65	.06
105	8.5	5.5	10.36	.05
95	9.9	6.8	11.40	.06
55	12.2	9.0	15.87	.08
25	24.9	11.5	23.25	.11

Sample Location UN-6 12-8-77

Depth Correction .0

	Radium		Radon	
Depth	DPS/CM^3	Var.	DPS/CM^3	Var.
0	12.0	3.6	5.67	.03
4	10.3	3.1	6.07	.02
9	10.8	2.5	5.81	.02
14	7.9	2.4	6.69	.02
19	10.2	2.5	6.59	.02
24	13.4	2.7	7.25	.02
34	12.4	3.0	7.59	.02
44	11.6	3.1	8.22	.03
54	12.7	3.2	8.07	.03
64	8.2	3.1	7.36	.03
74	9.8	3.5	8.94	.03
84	10.2	3.6	9.15	.03
89	10.1	3.6	8.96	.03

Sample Location UN-6 3-22-78

Depth Correction 2.0

	Radium		Radon	
Depth	DPS/CM^3	Var.	DPS/CM^3	Var.
2	10.7	1.3	5.65	.01
7	9.1	1.4	6.57	.01
12	9.9	1.6	7.00	.01
17	9.5	1.6	7.04	.01
22	8.8	1.7	7.54	.01
27	9.0	1.8	7.83	.01
32	10.9	1.9	7.93	.01
37	8.2	1.9	8.20	.02
47	10.5	2.0	8.17	.02
57	9.9	2.1	8.90	.02
67	10.3	2.2	9.55	.02
77	9.3	2.3	9.81	.02
89	12.5	2.3	10.18	.02

Sample Location KM-6 10-28-78

Depth Correction .0

	Radium		Radon	
Depth	DPS/CM^3	Var.	DPS/CM^3	Var.
0	22.8	4.9	20.79	.05
10	41.1	6.9	32.16	.07
20	39.3	7.6	31.84	.07
30	38.4	7.7	33.19	.08
40	36.0	7.7	35.33	.08
50	36.0	14.5	29.11	.14
60	38.5	14.2	31.50	.15
70	32.0	13.1	27.08	.13
70	31.0	13.1	28.11	.13
80	18.7	12.0	24.31	.12
90	20.9	11.8	21.41	.11
100	23.9	13.7	24.46	.13
110	43.7	17.3	44.67	.19
120	30.2	12.6	26.60	.12
130	13.5	8.0	13.16	.07
140	13.3	3.4	12.65	.03
150	14.7	3.4	14.12	.03
150	12.4	3.4	13.85	.03
160	17.6	3.4	15.00	.03
170	11.6	3.3	13.37	.03
180	14.5	3.4	14.91	.03
190	14.3	3.4	14.61	.03
200	12.9	3.3	13.54	.03
205	11.1	3.3	14.27	.03
205	11.5	3.3	13.87	.03
120	25.1	6.4	27.01	.06
110	44.4	8.6	43.28	.09
80	28.9	5.9	23.09	.05

Sample Location KM-6 10-29-78

Depth Correction .0

	Radium		Radon	
Depth	DPS/CM^3	Var.	DPS/CM^3	Var.
0	27.4	5.1	21.28	.05
10	38.9	7.0	32.76	.07
20	32.1	7.7	33.96	.08
30	34.3	15.8	33.91	.16
40	43.5	15.7	35.83	.16
50	30.3	14.6	30.01	.15
50	26.7	14.6	30.17	.14
60	29.0	14.3	29.31	.15
70	30.1	13.2	28.10	.13
80	29.7	12.0	24.01	.12
90	18.3	11.9	22.08	.11
100	30.7	13.9	24.85	.13
110	44.8	17.4	43.72	.19
120	31.4	12.5	26.69	.12
130	16.4	8.0	13.88	.07
140	14.7	3.4	12.43	.03
150	15.5	3.4	14.26	.03
160	16.7	3.5	15.42	.03
170	13.3	3.2	13.43	.03
170	11.6	3.3	13.32	.03
170	11.6	3.2	13.50	.03
180	13.8	3.4	15.34	.03
190	11.8	3.4	14.25	.03
200	11.0	3.3	13.83	.03
205	14.4	3.3	14.26	.03
80	25.9	12.2	24.28	.11
40	47.1	15.8	35.23	.16
0	25.4	5.0	21.14	.05

Sample Location KM-6 5-6-79

Depth Correction 1.0

	Radium		Radon	
Depth	DPS/CM^3	Var.	DPS/CM^3	Var.
1	25.0	10.8	21.86	.11
11	34.1	14.9	35.21	.17
21	36.5	15.5	31.11	.16
31	26.2	16.1	31.39	.16
41	25.0	16.0	32.90	.17
51	36.3	15.4	31.42	.16
61	28.4	14.6	31.06	.15
71	26.4	13.3	26.43	.14
81	18.9	11.7	21.96	.11
91	24.9	12.0	21.41	.12
101	23.3	15.2	29.91	.16
111	39.0	17.2	41.28	.20
121	14.6	9.8	13.79	.08
131	13.8	7.3	12.16	.06
151	14.8	6.8	14.24	.07
171	11.3	6.6	13.43	.06
191	14.7	6.5	12.91	.06
199	9.3	6.4	12.94	.06
101	23.3	15.2	29.54	.16
91	14.4	12.0	20.37	.11
81	23.7	11.8	22.42	.12

Sample Location KM-6 5-8-79

Depth Correction 1.0

	Radium		Radon	
Depth	DPS/CM^3	Var.	DPS/CM^3	Var.
1	27.1	10.9	23.86	.11
11	39.7	14.5	34.93	.16
21	33.8	15.2	30.72	.16
31	34.0	15.9	32.11	.16
41	32.6	15.8	32.63	.17
51	31.9	15.2	31.10	.16
61	31.1	14.8	31.20	.15
71	19.9	13.2	27.59	.14
81	23.9	11.6	21.81	.11
91	19.8	11.9	20.71	.12
101	22.9	14.9	28.33	.15
121	16.9	10.8	17.41	.10
161	12.0	6.5	12.70	.06
181	12.5	6.8	14.58	.07
200	13.5	6.5	13.21	.06
141	9.9	6.5	11.93	.06

Sample Location KM-6 5-10-79

Depth Correction 5.0

	Radium		Radon	
Depth	DPS/CM^3	Var.	DPS/CM^3	Var.
5	30.4	12.5	25.90	.13
10	42.3	14.3	32.49	.16
15	38.9	15.2	33.85	.17
20	30.4	14.9	28.76	.15
25	33.5	15.4	31.70	.16
30	---	---	30.44	.16
35	36.0	15.9	33.30	.17
45	27.9	15.1	29.98	.15
55	31.9	14.9	30.44	.15
65	28.3	14.0	28.48	.14
75	24.8	12.4	24.77	.13
85	22.1	11.6	20.80	.11
95	19.9	13.0	21.71	.12
100	28.3	14.4	26.81	.14
105	36.1	16.4	36.09	.18
110	32.6	17.4	44.15	.20
115	32.4	15.3	37.55	.17
120	11.8	10.7	17.13	.09
125	---	---	13.10	.07
135	11.3	6.9	12.17	.06
145	12.3	6.6	12.79	.06
155	15.0	6.8	14.60	.07
165	8.4	6.3	12.27	.06
175	9.7	6.6	14.59	.06
185	18.4	6.8	14.27	.07
195	11.3	6.4	13.01	.06
200	9.6	6.5	13.04	.06
125	13.3	8.7	13.06	.07
110	45.2	17.3	44.76	.20
30	26.9	15.6	30.12	.16

Sample Location KM-6 5-11-79

Depth Correction 1.0

	Radium		Radon	
Depth	DPS/CM^3	Var.	DPS/CM^3	Var.
1	25.7	10.6	20.41	.11
11	45.5	14.7	34.92	.16
21	32.4	15.1	28.75	.15
31	27.8	15.7	30.05	.16
41	36.1	15.6	31.43	.16
51	30.2	15.1	29.93	.15
61	21.7	14.4	29.47	.15
71	26.0	13.0	25.64	.13
81	26.8	11.5	21.93	.11
91	20.5	12.2	21.27	.12
101	17.0	14.9	28.34	.15
121	8.6	10.1	14.60	.08
141	9.9	6.7	12.51	.06
161	12.7	6.6	12.57	.06
181	17.3	6.9	15.40	.07
201	13.2	6.4	13.03	.06
111	39.8	17.1	42.93	.20

Sample Location KM-6 5-12-79

Depth Correction 1.0

	Radium		Radon	
Depth	DPS/CM^3	Var.	DPS/CM^3	Var.
1	20.9	11.0	21.65	.11
11	48.2	15.2	35.11	.17
21	33.1	15.2	29.78	.15
31	28.5	15.6	30.86	.16
41	32.0	15.7	30.66	.16
51	32.3	15.2	30.09	.16
61	27.4	14.6	30.59	.15
71	29.5	13.1	27.48	.13
81	19.4	11.7	21.34	.11
101	28.8	14.8	27.45	.15
121	18.5	10.7	16.49	.09
141	13.0	6.6	12.01	.06
161	12.0	6.5	12.46	.06
181	13.9	6.8	15.21	.07
201	11.0	6.4	12.37	.06
91	21.1	12.0	21.01	.11

Sample Location KM-6 5-14-79

Depth Correction 1.0

	Radium		Radon	
Depth	DPS/CM^3	Var.	DPS/CM^3	Var.
1	28.5	13.2	28.28	.14
11	42.9	15.2	33.59	.16
21	38.1	15.5	31.76	.16
31	33.5	15.9	32.47	.17
41	---	---	29.35	.15
51	30.7	15.2	31.76	.16
61	35.6	14.1	29.19	.14
71	28.8	12.5	25.34	.12
81	18.1	11.5	21.19	.11
91	19.7	12.7	21.88	.12
101	36.7	16.7	37.08	.18
111	40.1	15.7	37.75	.17
121	12.1	8.8	12.82	.07
141	16.5	6.7	12.72	.06
161	10.4	6.3	11.81	.06
181	16.0	6.8	14.74	.07
197	12.3	6.5	13.14	.06
146	18.9	6.8	13.37	.06
116	20.8	11.4	19.37	.10
106	38.8	17.3	44.07	.20
101	33.9	16.5	37.13	.18
96	16.7	14.1	24.94	.14
41	32.3	15.2	29.77	.15
21	38.1	15.6	30.27	.16
25	29.6	15.6	32.50	.16

Sample Location UN-7 12-8-77

Depth Correction .0

	Radium		Radon	
Depth	DPS/CM^3	Var.	DPS/CM^3	Var.
4	11.8	2.3	7.61	.02
9	10.9	1.9	7.64	.01
14	11.4	1.8	7.94	.01
19	13.0	2.0	8.95	.02
29	14.3	2.2	10.29	.02
39	14.4	2.2	9.67	.02
49	11.7	2.2	9.21	.02
59	8.0	2.1	8.85	.02
69	7.6	2.2	9.69	.02
79	9.7	2.2	9.82	.02
89	8.7	2.0	8.57	.02
99	4.2	1.7	6.81	.01
109	7.8	1.6	6.09	.01
119	6.9	1.7	6.38	.01
129	6.3	2.0	7.25	.01
139	7.0	2.8	9.98	.02
149	14.2	4.4	17.23	.04
159	---	---	22.54	.06
169	---	---	23.42	.07
179	---	---	23.31	.07
189	---	---	24.01	.07
199	---	---	19.25	.09

Sample Location UN-7 3-22-78

Depth Correction 12.0

	Radium		Radon	
Depth	DPS/CM^3	Var.	DPS/CM^3	Var.
12	7.3	1.7	7.08	.01
17	9.8	1.8	7.67	.01
22	13.5	2.0	9.35	.02
27	14.3	2.2	10.62	.02
32	9.6	2.1	8.96	.02
37	6.9	2.0	8.41	.02
42	9.4	1.9	8.15	.02
47	8.3	2.0	8.43	.02
52	6.2	2.0	8.74	.02
62	9.5	2.2	9.00	.02
72	11.7	2.3	10.16	.02
82	10.6	2.0	8.71	.02
92	6.3	1.6	6.19	.01
102	4.0	1.5	5.52	.01
112	6.7	1.7	6.23	.01
122	7.5	1.9	7.27	.01
132	10.2	2.6	9.07	.02
142	13.5	4.4	16.89	.04
152	27.6	12.9	31.75	.14
162	36.9	22.0	29.61	.23
172	29.4	14.5	31.32	.15
192	30.8	15.4	29.59	.15
212	38.5	18.5	38.36	.19

Sample Location KM-7 10-29-78

Depth Correction .0

	Radium		Radon	
Depth	DPS/CM^3	Var.	DPS/CM^3	Var.
0	17.5	3.0	14.72	.03
10	18.4	3.3	15.75	.03
20	15.5	3.4	15.23	.03
30	14.7	3.5	14.10	.03
40	16.3	3.9	16.76	.04
50	20.0	4.1	17.26	.04
50	17.4	4.1	17.19	.04
60	19.7	4.2	17.45	.04
60	21.6	4.2	17.60	.04
70	20.7	4.4	18.52	.04
80	20.9	4.3	18.05	.04
90	16.8	4.3	17.28	.04
100	20.5	4.3	16.66	.04
110	22.0	4.5	19.32	.04
120	20.4	4.6	20.11	.04
130	20.2	4.5	18.68	.04
140	15.6	4.3	18.03	.04
150	17.0	4.2	17.81	.04
160	17.1	4.2	17.97	.04
170	11.4	4.1	17.24	.04
180	18.3	4.0	16.93	.04
190	17.2	4.1	17.20	.04
200	21.0	4.2	17.60	.04
170	16.2	4.1	17.16	.04
140	16.3	4.3	18.15	.04
110	16.6	4.5	19.11	.04
80	22.3	4.4	18.39	.04
50	19.0	4.1	17.09	.04
20	16.2	3.5	15.36	.03
0	16.6	2.9	14.44	.03
0	17.8	2.9	14.73	.03
20	13.8	3.5	15.13	.03
50	18.9	4.1	17.08	.04
80	18.2	4.3	18.22	.04
110	14.0	4.5	19.56	.04
140	14.4	4.3	18.21	.04
170	14.5	4.1	17.34	.04

Sample Location KM-7 5-6-79

Depth Correction 9.0

	Radium		Radon	
Depth	DPS/CM^3	Var.	DPS/CM^3	Var.
9	19.4	6.7	15.66	.07
19	16.6	6.8	14.61	.07
29	15.7	6.9	13.97	.07
39	20.7	7.7	16.05	.08
49	17.7	8.2	16.95	.08
59	16.0	8.4	16.58	.08
69	17.6	8.8	18.14	.09
79	13.9	8.8	15.04	.08
89	19.1	8.7	16.20	.08
99	13.0	8.7	15.99	.08
109	20.9	9.2	18.80	.09
129	19.0	9.1	18.02	.09
149	17.4	8.5	18.20	.08
169	17.2	8.3	16.57	.08
189	15.9	8.4	17.42	.08
194	11.2	8.5	16.87	.08

Sample Location KM-7 5-8-79

Depth Correction 9.0

	Radium		Radon	
Depth	DPS/CM^3	Var.	DPS/CM^3	Var.
9	15.3	3.1	15.37	.03
29	16.0	6.9	14.13	.07
39	15.6	7.6	15.69	.08
49	17.8	8.1	15.87	.08
59	15.6	8.4	16.33	.08
69	15.1	8.8	16.07	.08
79	16.1	8.7	17.36	.08
89	18.3	8.5	16.95	.08
109	17.7	9.2	18.84	.09
129	11.3	9.0	18.14	.09
149	14.4	8.5	17.50	.08
169	11.8	8.3	17.43	.08
189	14.4	8.4	17.29	.08
99	15.1	8.7	16.34	.08
19	13.9	6.6	13.81	.07

Sample Location KM-7 5-10-79

Depth Correction 15.0

	Radium		Radon	
Depth	DPS/CM^3	Var.	DPS/CM^3	Var.
15	17.5	6.6	15.46	.07
25	18.0	6.6	14.27	.07
35	16.8	7.3	15.67	.07
45	14.0	8.1	17.12	.08
55	17.0	8.2	17.03	.08
65	19.1	8.6	17.47	.08
75	21.2	8.7	18.04	.09
85	18.9	8.6	17.50	.08
95	13.8	8.5	15.58	.08
105	22.7	9.0	18.43	.09
115	20.0	9.4	19.14	.09
145	19.5	8.8	17.02	.09
155	13.0	8.5	17.85	.08
175	16.6	8.2	16.66	.08
186	18.3	8.2	16.94	.08
15	20.8	8.6	15.80	.07

Sample Location KM-7 5-11-79

Depth Correction 15.0

	Radium		Radon	
Depth	DPS/CM^3	Var.	DPS/CM^3	Var.
15	15.6	6.7	15.93	.07
25	18.3	6.7	14.37	.07
35	11.8	7.3	15.19	.07
45	17.3	8.0	17.19	.08
55	20.3	8.3	16.78	.08
65	23.2	8.8	17.30	.09
75	17.6	8.8	18.30	.09
85	20.2	8.6	17.50	.09
95	11.0	8.5	15.54	.08
105	18.8	8.9	18.03	.09
115	13.8	9.2	19.11	.09
135	16.7	8.7	17.36	.09
155	15.5	8.4	17.66	.08
175	11.7	8.2	16.49	.08
188	17.0	8.3	16.94	.08

Sample Location KM-7 5-12-79

Depth Correction 15.0

	Radium		Radon	
Depth	DPS/CM^3	Var.	DPS/CM^3	Var.
15	22.4	6.6	15.46	.07
35	16.8	7.3	15.39	.07
45	15.4	7.9	16.67	.08
55	19.1	8.2	16.48	.08
65	16.3	8.6	17.40	.08
75	22.3	8.8	17.75	.09
85	15.9	8.7	15.93	.08
95	22.1	8.5	15.68	.08
105	19.1	8.9	17.70	.09
115	27.0	9.3	19.20	.09
135	19.8	8.7	17.56	.09
155	16.4	8.4	17.33	.08
175	21.5	8.2	16.70	.08
188	15.1	8.3	16.28	.08
25	17.7	6.8	13.76	.12

Sample Location KM-7 5-14-79

Depth Correction 15.0

	Radium		Radon	
Depth	DPS/CM^3	Var.	DPS/CM^3	Var.
15	17.4	6.8	16.53	.07
15	17.3	6.8	16.01	.07
15	13.8	6.8	16.45	.07
25	17.3	6.8	14.37	.07
35	15.2	7.4	15.37	.07
45	20.8	8.0	17.04	.08
55	13.6	8.4	16.60	.08
65	19.3	8.6	17.73	.09
75	17.7	8.8	18.58	.09
85	19.2	8.7	17.04	.08
95	19.0	8.6	16.00	.08
105	16.7	8.9	18.17	.09
115	17.2	9.3	19.20	.09
135	21.5	8.8	17.50	.09
155	14.4	8.5	17.27	.08
175	16.3	8.1	17.49	.08
189	13.5	8.3	17.41	.08
175	15.0	8.2	17.20	.08
175	16.5	8.2	16.83	.08
155	20.5	8.5	17.58	.08
155	17.9	6.8	17.58	.08
135	13.7	8.9	18.31	.09
135	16.6	8.8	18.34	.09
135	17.1	8.7	17.57	.09
115	21.7	9.3	19.36	.09
115	14.5	9.3	19.53	.09
115	18.0	9.2	19.66	.09
105	23.9	9.0	18.92	.09
105	18.1	9.1	18.89	.09
105	17.7	9.1	18.77	.09
95	17.6	8.6	15.97	.08
95	19.2	8.5	15.24	.08
85	17.5	8.8	18.08	.08
75	21.0	7.2	18.37	.09
75	13.5	7.3	18.40	.09
65	20.3	8.7	18.17	.09
65	18.4	8.7	18.64	.09
55	12.7	8.4	16.83	.08
55	19.1	8.4	17.22	.08
45	21.5	7.9	17.30	.08
45	12.0	8.1	16.74	.08
35	11.7	7.4	14.94	.07
25	12.8	6.8	13.97	.07
25	15.5	6.8	14.24	.07

Sample Location KM-7 5-16-79

Depth Correction 15.0

	Radium		Radon	
Depth	DPS/CM^3	Var.	DPS/CM^3	Var.
15	17.5	6.8	15.83	.07
25	14.1	6.7	14.00	.07
35	12.7	7.3	14.94	.07
45	19.8	8.1	16.95	.08
65	18.8	24.7	17.47	.08
75	19.0	5.5	18.23	.09
85	18.7	8.6	16.89	.08
105	17.7	9.0	18.48	.09
115	21.0	9.2	19.66	.09
125	15.5	9.0	19.13	.09
135	15.8	8.8	18.00	.08
155	16.2	8.5	18.03	.08
175	16.9	8.1	16.66	.08
188	16.0	8.3	17.11	.08
95	26.2	8.4	15.32	.08
55	15.6	8.4	16.78	.08

Sample Location UN-8 12-8-77

Depth Correction .0

	Radium		Radon	
Depth	DPS/CM^3	Var.	DPS/CM^3	Var.
0	26.0	7.9	23.78	.08
4	26.4	6.4	22.10	.06
9	23.8	5.0	19.99	.05
14	21.2	4.4	18.10	.04
19	18.2	4.3	17.14	.04
29	19.6	4.8	18.31	.05
39	25.7	5.8	21.21	.06
49	---	---	23.13	.11
59	---	---	19.90	.12
69	---	---	21.12	.10
79	---	---	19.56	.09
99	---	---	23.48	.10
119	---	---	22.29	.11
129	16.3	6.8	16.95	.07
139	14.0	6.0	14.64	.06
149	12.8	5.8	13.37	.05
159	19.4	6.4	13.69	.06
169	20.6	7.8	17.27	.08
179	20.4	10.0	20.26	.10
189	---	---	24.40	.14
199	---	---	25.16	.15
210	---	---	24.45	.12

Sample Location UN-8 3-23-78

Depth Correction 4.0

	Radium		Radon	
Depth	DPS/CM^3	Var.	DPS/CM^3	Var.
4	25.5	4.5	19.70	.04
4	28.5	4.5	19.71	.04
9	17.5	8.6	18.08	.08
9	20.3	8.6	17.83	.08
14	12.2	8.6	15.80	.08
19	17.4	9.0	17.07	.09
24	17.5	10.0	18.70	.10
29	21.2	11.4	23.02	.11
34	26.7	13.2	28.92	.14
44	21.9	15.1	35.13	.16
54	31.9	14.1	32.63	.15
64	17.7	11.5	26.06	.12
74	14.5	9.4	17.28	.09
84	28.0	11.5	25.93	.12
94	31.2	12.3	28.91	.13
104	33.7	11.6	27.14	.12
124	12.3	7.2	14.66	.07
144	11.1	7.0	14.40	.07
164	15.9	10.2	19.04	.10
184	45.6	17.6	42.65	.19
204	30.0	12.0	25.72	.12
209	19.7	10.4	19.68	.10
189	42.3	14.1	47.08	.13
184	42.4	17.6	43.76	.20
179	27.2	15.1	32.44	.16
174	21.2	13.3	25.53	.13
169	24.1	11.5	22.92	.11
164	17.6	10.3	19.57	.10
159	12.7	8.9	15.97	.08
154	14.3	7.8	13.30	.07
149	11.1	7.3	13.98	.07
144	15.5	7.0	14.16	.07

Sample Location UN-9 12-7-77

Depth Correction .0

	Radium		Radon	
Depth	DPS/CM^3	Var.	DPS/CM^3	Var.
0	10.3	2.2	7.03	.02
5	12.2	1.7	6.44	.01
15	9.9	1.2	5.93	.01
20	11.1	1.3	6.19	.01
25	8.5	1.4	6.63	.01
30	11.4	1.4	6.83	.01
35	10.5	1.5	6.91	.01
40	11.2	1.5	6.93	.01
45	10.6	1.5	7.02	.01
50	9.7	1.6	7.16	.01
55	8.9	1.6	7.49	.01
65	9.5	1.7	7.77	.01
75	9.7	1.7	7.90	.01
81	11.8	1.7	8.04	.01

Sample Location UN-9 3-21-78

Depth Correction 22.0

	Radium		Radon	
Depth	DPS/CM^3	Var.	DPS/CM^3	Var.
22	10.6	1.2	5.70	.01
27	8.0	1.2	5.48	.01
32	8.7	1.2	5.45	.01
37	8.8	1.3	5.78	.01
42	7.9	1.3	5.61	.01
47	10.4	1.3	5.75	.01
49	8.2	1.4	6.35	.01
54	10.6	1.5	6.59	.01
59	9.4	1.5	6.83	.01
64	9.1	1.5	6.75	.01
69	9.9	1.6	6.87	.01
74	9.1	1.6	6.94	.01
79	9.5	1.6	7.13	.01
82	6.9	1.6	7.58	.01

Sample Location UN-9B 5-5-79

Depth Correction .0

	Radium		Radon	
Depth	DPS/CM^3	Var.	DPS/CM^3	Var.
0	8.2	.8	5.21	.00
10	7.5	.9	5.72	.00
20	10.3	.9	6.09	.00
30	10.1	1.0	6.50	.01
40	8.7	1.0	6.64	.01
50	6.9	1.1	6.93	.01
60	9.5	1.1	7.22	.01
80	8.3	1.1	6.91	.01
90	9.2	1.2	7.40	.01
100	8.1	1.2	7.31	.01
120	10.4	1.3	8.33	.01
140	6.9	1.3	8.68	.01
160	7.1	1.3	8.63	.01
180	11.2	1.4	9.06	.01
200	8.7	1.4	9.07	.01
220	6.7	1.4	8.51	.01

Sample Location UN-9B 5-9-79

Depth Correction 34.0

	Radium		Radon	
Depth	DPS/CM^3	Var.	DPS/CM^3	Var.
34	7.6	.8	5.47	.00
44	9.2	.9	6.64	.01
54	10.3	1.0	6.75	.01
64	10.0	1.1	6.86	.01
74	9.8	1.1	7.09	.01
84	7.7	1.1	7.03	.01
94	9.5	1.2	7.39	.01
104	8.4	1.2	6.94	.01
114	9.2	1.2	7.43	.01
124	9.7	1.3	8.07	.01
134	8.1	1.3	8.41	.01
154	11.0	1.3	8.75	.01
174	8.8	1.4	9.04	.01
194	9.5	1.4	9.15	.01

Sample Location UN-9B 5-11-79

Depth Correction 36.0

	Radium		Radon	
Depth	DPS/CM^3	Var.	DPS/CM^3	Var.
36	8.2	.8	5.54	.00
46	10.1	.9	6.44	.01
56	9.9	1.0	6.55	.01
66	8.1	1.1	6.79	.01
76	9.1	1.1	7.00	.01
86	10.0	1.1	7.08	.01
96	9.3	1.1	7.11	.01
106	8.5	1.1	6.65	.01
116	9.3	1.2	7.54	.01
126	9.1	1.2	8.19	.01
156	11.1	1.3	8.54	.01
176	8.5	1.3	8.51	.01
196	7.1	1.4	8.80	.01
216	9.7	1.4	9.08	.01
236	8.0	1.3	7.96	.01

Sample Location UN-9B 5-13-79

Depth Correction 36.0

	Radium		Radon	
Depth	DPS/CM^3	Var.	DPS/CM^3	Var.
36	9.8	.8	5.67	.00
46	8.9	.9	6.38	.01
56	9.3	1.0	6.54	.01
66	9.5	1.0	6.74	.01
76	7.1	1.1	6.95	.01
86	8.5	1.1	6.98	.01
96	8.8	1.1	7.31	.01
106	9.2	1.1	6.84	.01
116	9.0	1.2	7.45	.01
126	9.5	1.3	8.36	.01
136	9.3	1.3	8.41	.01
156	11.3	1.3	8.57	.01
176	9.1	1.3	8.91	.01
196	10.9	1.4	8.99	.01
216	10.3	1.4	8.59	.01
236	9.0	1.4	8.01	.01

Sample Location UN-9B 5-15-79

Depth Correction 37.0

	Radium		Radon	
Depth	DPS/CM^3	Var.	DPS/CM^3	Var.
127	10.6	1.3	8.10	.01
137	8.6	1.3	8.28	.01
157	7.3	1.3	8.72	.01
177	8.6	1.4	8.70	.01
197	8.1	1.4	9.01	.01
217	8.4	1.4	8.63	.01
237	7.9	1.4	7.96	.01
107	9.0	.8	6.91	.00
67	9.5	1.0	6.74	.01
57	9.3	.4	6.65	.01
47	8.8	.9	6.37	.01
87	8.0	1.1	6.96	.01

Sample Location UN-10 12-8-77

Depth Correction .0

	Radium		Radon	
Depth	DPS/CM^3	Var.	DPS/CM^3	Var.
4	14.0	2.7	10.65	.02
9	14.8	2.2	10.30	.02
14	13.5	1.9	9.68	.02
19	11.7	1.9	9.68	.02
29	14.2	2.0	9.82	.02
39	9.9	2.1	9.91	.02
49	13.5	2.1	10.08	.02
59	12.0	2.1	9.98	.02
69	8.6	2.1	9.61	.02
79	11.6	2.3	11.42	.02
89	11.7	2.4	11.57	.02
99	8.8	2.4	10.92	.02
109	11.7	2.4	11.00	.02
119	11.1	2.6	11.49	.02
129	13.1	2.8	12.19	.02
139	10.9	3.0	13.35	.03
149	17.8	3.2	14.19	.03
159	13.9	3.2	14.47	.03
169	11.6	3.0	13.64	.03
179	12.6	2.9	12.62	.03
189	11.7	2.9	12.86	.03
199	13.0	2.9	13.10	.03
209	15.0	2.8	13.04	.03
213	10.0	2.8	12.97	.03

Sample Location UN-10 3-23-78

Depth Correction 3.0

	Radium		Radon	
Depth	DPS/CM^3	Var.	DPS/CM^3	Var.
8	7.9	1.7	7.32	.01
13	9.4	1.7	7.49	.01
18	11.0	1.8	7.50	.01
23	11.9	1.9	8.12	.01
28	9.9	1.9	8.41	.02
33	9.3	2.0	9.23	.02
38	11.1	2.0	9.19	.02
43	10.0	2.0	8.97	.02
53	7.5	2.0	8.54	.02
63	9.6	2.1	9.64	.02
73	12.2	2.3	9.89	.02
83	8.9	2.4	10.88	.02
93	8.0	2.3	8.82	.02
103	8.7	2.3	8.63	.02
113	10.6	2.4	9.24	.02
123	13.2	2.6	10.61	.02
133	13.7	2.9	12.00	.02
143	16.1	3.1	13.55	.03
153	13.5	3.0	13.24	.03
163	10.9	2.8	11.27	.02
173	6.3	2.6	10.74	.02
183	10.3	2.6	10.57	.02
193	12.3	2.7	11.78	.02
213	12.2	3.3	11.34	.03
213	11.2	2.6	11.47	.02
213	12.8	2.6	11.22	.02
213	10.7	2.6	11.35	.02
213	8.6	2.6	10.97	.02

Sample Location UN-11 12-8-77

Depth Correction .0

	Radium		Radon	
Depth	DPS/CM^3	Var.	DPS/CM^3	Var.
4	8.2	.7	5.43	.00
9	8.4	.5	4.98	.00
14	10.4	.5	5.18	.00
19	7.6	.5	5.53	.00
29	10.8	1.4	6.78	.01
39	11.5	1.7	8.25	.01
49	11.1	1.9	8.71	.02
59	13.5	2.0	9.23	.02
69	12.7	2.1	9.61	.02
79	13.8	2.1	10.08	.02
89	13.8	2.1	9.94	.02

Sample Location UN-11 3-22-78

Depth Correction 18.0

	Radium		Radon	
Depth	DPS/CM^3	Var.	DPS/CM^3	Var.
18	7.7	1.1	6.31	.01
23	5.9	1.2	6.45	.01
28	9.0	1.4	6.65	.01
33	6.9	1.5	7.29	.01
38	11.1	1.6	7.90	.01
43	8.5	1.8	8.15	.01
48	9.9	1.8	8.52	.02
53	8.9	1.9	8.75	.02
58	9.8	1.9	8.66	.02
68	11.9	2.0	8.41	.02
78	9.5	2.0	8.79	.02
89	13.1	2.1	8.83	.02

Sample Location UN-12 10-26-78

Depth Correction .0

	Radium		Radon	
Depth	DPS/CM^3	Var.	DPS/CM^3	Var.
0	29.9	4.4	20.78	.05
10	30.5	4.8	20.96	.05
20	18.4	4.7	17.15	.04
30	26.2	5.1	20.45	.05
40	28.1	5.6	23.79	.05
50	26.4	5.7	23.20	.05
60	22.7	5.5	20.71	.05
60	23.3	5.5	20.49	.05
70	17.0	5.8	22.86	.05
80	25.1	6.0	24.69	.06
90	23.3	5.9	24.57	.06
100	23.6	5.8	19.70	.05
110	22.6	6.4	23.49	.06
120	28.3	7.4	31.16	.07
130	29.9	7.6	32.61	.08
140	28.7	6.9	27.27	.07
150	28.0	6.4	26.56	.06
160	23.0	5.6	20.62	.05
170	21.6	5.4	19.23	.05
180	28.0	6.1	25.61	.06
190	32.3	6.5	27.67	.06
200	36.2	5.9	25.73	.06
210	29.0	4.7	15.97	.04
217	22.2	4.3	14.58	.03
70	26.9	5.8	21.93	.05

Sample Location UN-12 10-30-78

Depth Correction .0

	Radium		Radon	
Depth	DPS/CM^3	Var.	DPS/CM^3	Var.
0	33.4	9.7	26.32	.11
10	26.0	10.0	23.47	.10
20	21.3	9.7	19.62	.09
30	25.9	10.5	21.52	.10
40	29.4	11.7	25.35	.12
50	28.3	11.9	24.82	.12
60	26.0	11.4	21.82	.11
70	24.9	11.9	24.22	.12
80	24.4	12.5	25.89	.13
90	18.7	12.3	26.58	.13
100	15.3	12.0	23.00	.12
110	20.8	13.4	25.93	.13
120	34.6	15.7	34.72	.16
130	33.7	15.9	38.24	.16
140	30.0	15.0	31.84	.15
150	27.8	13.8	29.60	.14
160	24.1	12.7	25.74	.13
170	21.8	12.5	24.77	.12
180	29.9	14.0	31.48	.15
190	37.5	14.8	33.59	.15
200	32.6	13.7	31.18	.14
210	23.6	11.4	22.51	.11
130	31.1	15.9	34.22	.16
90	22.9	12.2	25.14	.12
30	21.3	10.6	21.54	.10
0	29.9	9.2	22.39	.10
90	20.0	12.0	25.15	.12

Sample Location UN-12 5-10-79

Depth Correction 3.0

	Radium		Radon	
Depth	DPS/CM^3	Var.	DPS/CM^3	Var.
3	33.9	9.0	20.47	.10
13	24.4	9.0	16.53	.08
23	27.2	9.3	15.96	.08
33	25.9	10.7	21.03	.11
43	32.9	11.7	24.07	.12
53	27.3	11.6	22.39	.11
63	19.7	11.4	20.97	.11
73	26.4	12.1	23.67	.12
83	24.8	12.4	24.70	.12
93	20.7	11.8	22.37	.12
103	17.1	12.0	20.95	.11
123	29.0	15.4	32.28	.16
143	26.1	13.5	26.74	.14
163	22.6	11.2	20.22	.11
183	38.1	12.9	29.07	.14
203	34.6	11.2	21.78	.11
133	28.3	14.9	30.14	.15
113	27.0	13.8	25.22	.14

Sample Location UN-12 5-12-79

Depth Correction 3.0

	Radium		Radon	
Depth	DPS/CM^3	Var.	DPS/CM^3	Var.
3	31.9	9.3	21.10	.10
13	25.2	9.0	17.19	.09
23	22.7	9.6	17.63	.09
33	24.4	11.0	22.36	.11
43	34.8	11.7	25.29	.12
53	24.5	11.7	22.96	.12
63	19.9	11.4	20.40	.11
73	27.8	12.1	24.17	.12
83	25.9	12.4	24.75	.13
93	19.2	11.8	21.77	.11
103	13.9	12.0	21.12	.12
123	36.4	15.5	31.78	.16
143	28.8	13.4	25.85	.13
163	25.9	11.0	20.49	.11
183	33.0	12.8	27.75	.13
203	30.4	10.8	21.22	.10
214	23.4	8.8	14.80	.08
113	18.0	13.8	25.74	.14

Sample Location UN-12 5-14-79

Depth Correction 3.0

	Radium		Radon	
Depth	DPS/CM^3	Var.	DPS/CM^3	Var.
103	18.3	12.0	20.06	.12
123	30.1	15.6	32.43	.16
143	25.5	13.8	26.65	.14
163	24.5	11.5	21.01	.11
183	35.5	13.5	29.58	.14
203	33.0	11.2	21.74	.11
93	26.7	11.9	21.65	.11
43	34.9	11.9	25.07	.12
3	34.1	9.3	20.80	.10

Sample Location UN-12 5-15-79

Depth Correction 3.0

	Radium		Radon	
Depth	DPS/CM^3	Var.	DPS/CM^3	Var.
3	29.2	9.4	20.77	.10
13	---	---	17.89	.09
23	24.5	9.7	17.04	.09
33	24.1	10.9	21.64	.11
43	25.8	12.0	25.34	.12
53	25.9	11.8	23.65	.12
63	21.2	11.5	21.26	.11
73	22.1	12.1	24.61	.12
83	22.9	12.4	25.83	.13
93	29.4	11.8	21.17	.11
103	28.0	12.1	21.52	.12
123	31.1	15.7	32.34	.16
143	26.4	14.1	28.75	.14
163	26.3	11.7	22.93	.11
183	37.8	13.6	30.75	.14
203	27.4	11.7	23.33	.11
73	15.5	12.3	25.37	.12
43	26.8	11.9	25.41	.12
13	25.5	9.2	18.82	.09
3	29.9	9.9	19.68	.10

Sample Location UN-12 5-16-79

Depth Correction 3.0

	Radium		Radon	
Depth	DPS/CM^3	Var.	DPS/CM^3	Var.
3	34.9	9.7	22.17	.10
8	27.6	9.3	19.76	.09
13	23.3	9.3	18.32	.09
23	21.5	9.7	17.92	.09
28	23.2	10.4	20.14	.10
33	23.3	11.0	21.73	.11
43	25.5	12.1	25.84	.13
53	23.5	11.9	24.23	.12
63	16.4	11.7	22.30	.12
73	28.2	12.5	26.23	.13
83	24.5	12.8	26.82	.13
93	15.9	11.9	22.35	.12
98	18.3	12.0	20.83	.12
103	21.9	12.6	22.69	.12
108	25.0	13.3	24.67	.13
113	20.0	14.5	29.19	.15
123	31.3	16.2	34.51	.17
133	26.4	15.7	33.33	.17
143	22.3	14.7	30.31	.15
153	21.7	13.3	25.64	.13
163	23.1	12.7	25.04	.13
173	25.9	13.3	25.47	.13
183	28.8	15.0	33.33	.16
193	36.6	14.8	33.02	.16

Sample Location UN-13 10-26-78

Depth Correction .0

	Radium		Radon	
Depth	DPS/CM^3	Var.	DPS/CM^3	Var.
0	16.5	2.7	10.98	.02
10	24.5	3.7	15.58	.03
20	24.2	7.7	20.61	.08
30	29.0	5.0	21.01	.05
40	27.3	4.9	19.20	.04
50	23.6	4.8	18.41	.04
60	24.8	5.1	20.48	.05
70	25.6	5.3	20.72	.05
80	28.8	5.4	23.59	.05
90	22.5	5.1	19.15	.05
100	25.2	5.0	20.41	.05
110	16.3	5.0	19.27	.05
120	17.4	5.0	18.87	.05
130	21.6	5.1	20.91	.05
140	20.7	5.3	21.96	.05
150	21.8	5.4	20.81	.05
160	23.2	5.8	24.69	.06
170	24.4	6.1	25.93	.06
180	25.2	6.2	24.39	.06
190	24.4	6.5	26.13	.06
210	33.6	7.3	32.28	.07
210	29.0	7.4	29.31	.07
215	31.2	7.7	31.45	.07
70	27.7	5.3	20.54	.05

Sample Location UN-13 10-30-78

Depth Correction .0

	Radium		Radon	
Depth	DPS/CM^3	Var.	DPS/CM^3	Var.
0	18.2	6.1	12.58	.06
10	26.2	7.9	16.02	.08
20	31.0	9.7	21.55	.10
30	21.8	10.1	20.85	.10
40	16.4	10.0	20.19	.10
50	22.4	9.8	18.62	.09
60	21.1	10.5	21.06	.10
70	23.0	10.7	21.23	.10
80	27.2	10.7	22.24	.10
90	22.7	10.3	20.65	.10
100	21.1	10.2	20.52	.10
110	17.6	10.1	19.60	.10
120	24.1	10.2	19.37	.10
130	19.4	10.7	22.28	.10
140	25.0	10.8	22.15	.11
150	26.4	11.1	23.09	.11
160	20.9	12.1	25.70	.12
170	33.0	12.4	26.66	.12
180	25.1	12.6	24.32	.12
190	27.2	13.8	29.34	.14
200	24.9	14.9	31.43	.15
210	28.0	15.2	31.42	.16
20	30.5	9.6	21.28	.10
10	25.0	8.1	16.63	.08
0	18.1	6.0	12.19	.06

Sample Location UN-13 5-10-79

Depth Correction 3.0

	Radium		Radon	
Depth	DPS/CM^3	Var.	DPS/CM^3	Var.
3	18.6	5.7	11.14	.05
3	13.9	5.8	11.89	.06
13	25.9	7.5	15.30	.07
23	25.5	9.0	18.97	.09
33	24.7	9.2	17.85	.09
43	26.1	9.6	18.87	.09
53	25.5	9.9	19.08	.10
63	23.2	10.7	21.65	.11
73	22.5	11.1	23.14	.11
83	21.1	10.6	19.35	.10
93	21.9	10.4	20.30	.10
103	29.3	10.5	20.71	.10
113	21.6	10.4	18.75	.10
123	16.9	10.6	20.37	.10
143	19.9	11.0	21.00	.11
163	20.6	12.3	25.96	.13
183	16.1	12.8	23.33	.13
203	28.4	15.2	30.89	.16
211	27.5	15.5	30.62	.16

Sample Location UN-13 5-12-79

Depth Correction 3.0

	Radium		Radon	
Depth	DPS/CM^3	Var.	DPS/CM^3	Var.
3	21.0	5.8	11.31	.06
13	21.5	7.6	14.98	.07
23	27.4	9.0	19.08	.09
33	24.8	9.1	16.98	.09
43	25.3	9.6	19.42	.09
53	23.0	10.0	20.02	.10
63	27.6	10.8	21.19	.11
73	27.2	11.1	23.21	.11
83	18.0	10.5	19.59	.10
93	23.0	10.6	21.24	.10
103	19.6	10.4	20.82	.10
123	20.0	10.5	20.12	.10
143	23.0	11.0	20.63	.11
163	20.8	12.2	25.50	.13
183	21.1	12.9	24.10	.13
203	33.2	15.0	32.71	.15
209	26.7	15.2	29.93	.16

Sample Location UN-13 5-14-79

Depth Correction 6.0

	Radium		Radon	
Depth	DPS/CM^3	Var.	DPS/CM^3	Var.
6	21.2	6.4	13.17	.06
16	28.0	8.1	16.56	.08
26	29.6	9.3	19.33	.09
36	25.5	9.2	17.57	.09
46	22.4	9.7	18.57	.09
46	---	---	18.60	.09
56	---	---	20.62	.10
66	25.0	10.9	20.32	.10
76	30.2	11.2	23.46	.11
86	19.5	10.5	20.20	.10
96	22.1	10.5	20.86	.10
106	16.9	10.4	19.54	.10
106	13.9	10.4	19.81	.10
126	---	---	21.32	.11
146	19.1	10.9	20.89	.11
166	22.5	12.4	25.54	.13
186	26.6	13.2	24.34	.13
206	27.3	15.1	28.18	.15

Sample Location UN-13 5-15-79

Depth Correction 6.0

	Radium		Radon	
Depth	DPS/CM^3	Var.	DPS/CM^3	Var.
6	22.0	6.5	13.45	.07
16	25.1	8.1	16.52	.08
26	27.0	9.1	18.79	.09
36	27.5	9.2	17.76	.09
46	24.5	9.6	18.03	.09
66	25.0	10.9	20.69	.11
86	19.1	10.4	19.92	.10
96	24.3	10.6	20.36	.10
106	19.7	10.4	19.55	.10
116	23.4	10.4	20.19	.10
126	19.8	10.8	20.32	.10
146	24.1	10.9	21.39	.11
166	25.6	12.5	25.02	.13
186	---	---	24.97	.13
206	23.2	15.1	30.02	.15
186	26.0	13.2	24.75	.13
76	24.4	11.2	23.96	.11
56	23.0	10.3	20.14	.10

DISTRIBUTION

No. of Copies

OFFSITE

A. A. Churm
DOE Patent Division
9800 S. Cass Avenue
Argonne, IL 60439

210 U. S. Nuclear Regulatory Commission
Division of Technical Information and Document Control
7920 Norfolk Avenue
Bethesda, MD 20014

2 DOE Technical Information Center
Washington, D. C. 20545

250 William E. Thompson
Technology Assessment Branch
Division of Fuel Cycle and Material Safety
U. S. Nuclear Regulatory Commission
Washington, D. C. 20555

William E. Gray, Manager
Environmental Engineering
Anaconda Company
660 Bannock Street
Denver, CO 80204

Edward E. Kennedy, Manager
Environmental Engineering
United Nuclear-Homestake Partners Corporation
P. O. Box 98
Grants, NM 87020

H. J. Abbiss, Vice President
Environmental and Safety Services
United Nuclear Corporation
Mining and Milling Division
P. O. Box 3951
Albuquerque, NM 87110

No. of Copies

OFFSITE (continued)

M. H. Momeni
Division of Environmental Impact Studies
Argonne National Laboratory
Argonne, IL 60439

James E. Cleveland
Environmental Engineer
Kerr-McGee Nuclear Corporation
P. O. Box 218
Grants, NM 87020

Tom Buhl
Regional Ore Office
State of New Mexico
Health and Social Services Department
Environmental Improvement Division
P. O. Box 968
Santa Fe, NM 87503

Arthur Miller, Vice President
Reserve Oil and Minerals Corp.
Suite 308
20 First Plaza
Albuquerque, NM 87102

Jim Roselle
Ranchers Exploration and Development Corporation
P. O. Box 6217
Albuquerque, NM 87107

Jack Rothfleisch
U. S. Nuclear Regulatory Commission
Nuclear Materials, Safety, and Safeguards
Washington, D. C. 20555

William J. Shelley, Director
Regulation and Control
Kerr-McGee Nuclear Corporation
2205 McGee Tower
Oklahoma City, OK 73125

DISTRIBUTION (continued)

No. of Copies

OFFSITE (continued)

10 Laura E. Santos
Office of Nuclear Regulatory Research
Division of Safeguards, Fuel Cycle and Environmental Research
Mail Stop 1130SS
Washington, D. C. 20555

K. K. Nielson
Ford, Bacon & Davis Utah, Inc.
P. O. Box 8009
Salt Lake City, UT 84108

No. of Copies

ONSITE

50 W. I. Enderlin
W. D. Felix
J. A. Glissmeyer
W. B. Silker (12)
R. W. Perkins (6)
L. C. Schwendiman
V. W. Thomas
W. R. Wiley
N. A. Wogman
J. N. Hartley
P. C. Heasler (6)
P. O. Jackson
J. M. Nielsen
P. L. Koehmstadt
G. A. Sehmel
R. J. Serne
C. W. Thomas
L. G. Faust
J. S. Fruchter
Technical Information (5)
Publishing Coordination (2)